Journal of Medicinal Chemistry

Article

pubs.acs.org/jmc

Synthesis and Biological Evaluation of Urea Derivatives as Highly Potent and Selective Rho Kinase Inhibitors

Yan Yin,[†,#] Li Lin,[§] Claudia Ruiz,[§] Susan Khan,[§] Michael D. Cameron,[§,¥] Wayne Grant,[‡] Jennifer Pocas,[‡] Nibal Eid,[‡] HaJeung Park,[∞] Thomas Schröter,[‡] Philip V. LoGrasso,*[,‡,¥] and Yangbo Feng*[,†]

[†]Medicinal Chemistry; [‡]Discovery Biology; [∞]Crystallography/Modeling Facility; [§]Drug Metabolism and Pharmacokinetics, Translational Research Institute, and [¥]Department of Molecular Therapeutics, The Scripps Research Institute, Scripps Florida, 130 Scripps Way, #2A1, Jupiter, Florida 33458, United States

Supporting Information

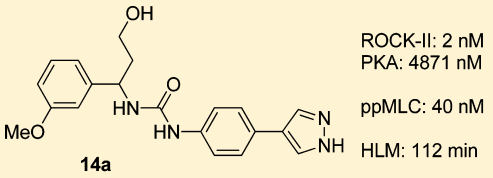

14a

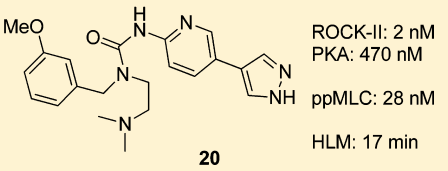

20

ABSTRACT: RhoA and its downstream effector ROCK mediate stress fiber formation and cell contraction through their effects on the phosphorylation of myosin light chain (MLC). Inhibition of the RhoA/ROCK pathway has proven to be a promising strategy for several indications such as cardiovascular disease, glaucoma, and inflammatory disease. In 2010, our group reported urea-based ROCK inhibitors as potential antiglaucoma agents. These compounds showed potent IC_{50} values in enzymatic and cell-based assays and significant intraocular pressure (IOP)-lowering effects in rats (~7 mmHg).[22] To develop more advanced ROCK inhibitors targeting various potential applications (such as myocardial infarction, erectile dysfunction, multiple sclerosis, etc.) in addition to glaucoma, a thorough SAR for this urea-based scaffold was studied. The detailed optimization process, counter-screening, and in vitro and in vivo DMPK studies are discussed. Potent and selective ROCK inhibitors with various in vivo pharmacokinetic properties were discovered.

INTRODUCTION

Rho-associated coiled-coil protein kinase (ROCK) is a serine/threonine protein kinase from the AGC kinase family with isoforms identified as ROCK-I (or ROCKβ) and ROCK-II (or ROCKα).[1] When activated by small GTP-bound RhoA, ROCK induces phosphorylation of myosin light chain (MLC) in a dual way by increasing MLC bis-phosphorylation directly and by preventing its dephosphorylation through inhibition of the MLC phosphatase thereby resulting in cellular contraction.[2] The contractile effect regulates a variety of physiological processes including smooth muscle contraction,[2] blood pressure,[3] endothelial permeability,[4] IOP,[5] and cellular migration.[6] Accumulating evidence suggests that RhoA/ROCK signaling cascade is involved in various diseases that involve contractile processes, such as multiple sclerosis,[7] pulmonary hypertension,[8] cardiovascular diseases,[3,9] glaucoma,[5] erectile dysfunction,[10,11] and cancer.[6]

ROCK has attracted numerous and diverse interests, and many ROCK inhibitors have been reported.[12−21] We have previously reported a urea-based ROCK inhibitor **1**[22] (Figure 1) which showed excellent enzymatic and cellular potency, high selectivity, good aqueous solubility, good porcine corneal penetration, appropriate DMPK properties, and significant IOP lowering effects in rat eyes. Molecular modeling studies showed that the pyrazole group binds to the hinge with two H-bonds, and the urea carbonyl group H-bonds to the side chain of Lys121 (Figure 1). Docking studies demonstrated that hydrophobic interactions between the benzyl moiety of compound **1** and the hydrophobic pocket of ROCK-II located under the P-loop appeared to be a key element responsible for its high potency and selectivity. In addition, H-bonds between the protonated tertiary amine and the carboxylate side chain of Asp176 of ROCK-II (Figure 1) also contributed to high potency and selectivity, and the tertiary amine side chain enhanced the aqueous solubility of inhibitor **1**.[22]

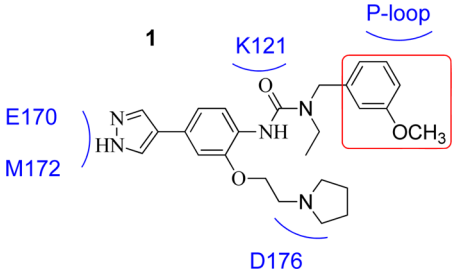

Figure 1. A previously disclosed urea-based ROCK inhibitor (**1**) and its key interactions in the ATP site of ROCK-II.[27] In addition to hinge binding to residues E170 and M172, the other three interactions also contributed to the high potency of this urea-based ROCK inhibitor.

Received: January 13, 2013

   dx.doi.org/10.1021/jm400062r | J. Med. Chem. XXXX, XXX, XXX−XXX

Among the several scaffolds developed in our laboratories,[22−31] the urea chemotype is the most interesting. In addition to furnishing highly selective and potent ROCK inhibitors,[22] it also provides many diversification points for structure−activity relationship (SAR) studies and for modifying the inhibitor's overall pharmaceutical properties, such as substitution to the middle phenyl ring, alkylation to both NH moieties of the urea group, substitution to the benzyl methylene position, and mono- or multisubstitution to the benzyl phenyl ring (Figure 1). Moreover, the middle phenyl ring may be replaced by a heteroaromatic group, and the tail benzyl moiety may be replaced by other saturated or unsaturated systems. Here we report extensive SAR studies on all these positions in a continuing effort to develop highly efficacious and pharmaceutically viable ROCK inhibitors from the urea scaffold. These SAR studies are aimed at understanding key elements of the ROCK ATP-binding pocket and at providing information to guide the design of ROCK inhibitors with diversified properties.

CHEMISTRY

The preparation of unsubstituted ROCK inhibitor **5** is outlined in Scheme 1. Urea, carbamate, or amide intermediates (**4a−f** and **4h−p**) were quickly accessed through a coupling reaction between 1-bromo-4-isocyanobenzene and a primary amine (to form a urea) or an alcohol (to form a carbamate) in DCM, or a condensation between 4-bromoaniline and a carboxylic acid (to produce the carboxyl amide intermediate) in the presence of HATU in DMF. The target compounds **5a−p** were prepared through a Suzuki coupling reaction between intermediate **4** and boronic acid pinacol ester catalyzed by $Pd(PPh_3)_4$. The final obtained ROCK inhibitors were all purified by preparative reverse-phase HPLC.

Scheme 1. Synthesis of Inhibitors 5a−p[a]

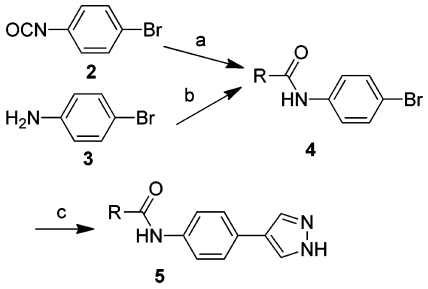

[a]Reagents and conditions: (a) Primary amine or alcohol; (b) acid, HATU, DIEA, DMF; (c) boronic acid pinacol ester, $Ph(PPh_3)_4$, K_2CO_3, dioxane/H_2O (4:1), 95 °C.

To make compounds **8a−f** that possess a substitution on the urea NH group from aniline, commercial or in-house-prepared N-substituted 4-bromoaniline **6** was reacted with 1-(isocyanomethyl)-3-methoxybenzene in DCM to form the urea intermediate **7**. A Suzuki coupling was then applied (Scheme 2) to furnish the final inhibitor **8**.

Scheme 2. Synthesis of Inhibitors 8a−f[a]

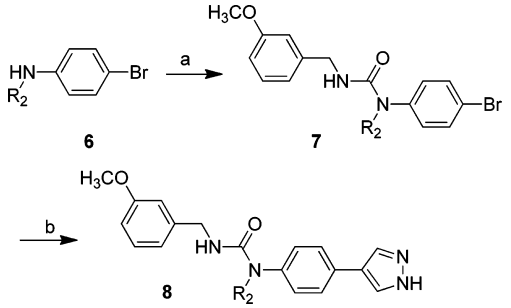

[a]Reagents and conditions: (a) 1-(Isocyanomethyl)-3-methoxybenzene, DCM; (b) boronic acid pinacol ester, $Ph(PPh_3)_4$, K_2CO_3, dioxane/H_2O (4:1), 95 °C.

A short route was used to synthesize inhibitor **12** which possessed a substitution on the urea NH group from benzylamine (Scheme 3). Treatment of a substituted benzaldehyde **9** with a primary amine, followed by $NaBH_4$ reduction, gave the secondary amine **10**. This amine was reacted with 1-bromo-4-isocyanobenzene in DCM to furnish the bromide intermediate **11**. Finally, compound **12** was formed via a Suzuki reaction and purified by preparative HPLC.

Scheme 3. Synthesis of Inhibitors 12a−n[a]

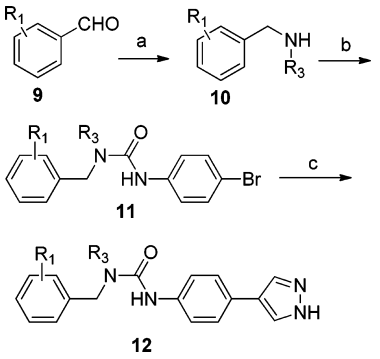

[a]Reagents and conditions: (a) (i) R_3-NH_2, MeOH, r.t; (ii) $NaBH_4$, 0 °C; (b) 1-bromo-4-isocyanatobenzene, DCM; (c) boronic acid pinacol ester, $Ph(PPh_3)_4$, K_2CO_3, dioxane/H_2O (4:1), 95 °C.

Application of α-position-substituted benzylamines led to Rock inhibitor **14**. As shown in Scheme 4, a urea formation between 4-bromoisocyanobenzene and a selected α-branched benzylamine gave intermediate **13**, which was subjected to a $Ph(PPh_3)_4$-catalyzed Suzuki coupling reaction (Scheme 4) to yield the final product **14**.

Scheme 4. Synthesis of Inhibitors 14a−d[a]

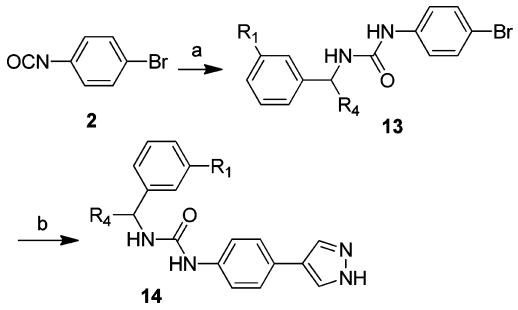

[a]Reagents and conditions: (a) α-Substituted benzylamines, DCM; (b) boronic acid pinacol ester, $Ph(PPh_3)_4$, K_2CO_3, dioxane/H_2O (4:1), 95 °C.

Inhibitors with substitutions on both the middle phenyl ring and on a urea NH group were synthesized as shown in Scheme 5. A S_NAr reaction was first used to furnish the 4-bromo-

dx.doi.org/10.1021/jm400062r | J. Med. Chem. XXXX, XXX, XXX−XXX

Scheme 5. Synthesis of Inhibitors 19a and 19b[a]

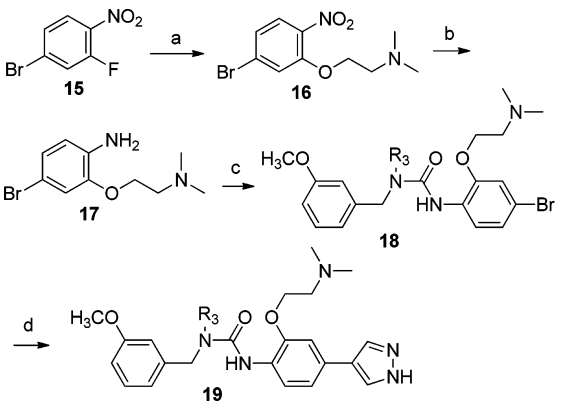

[a]Reagents and conditions: (a) 2-(Dimethylamino)ethanol, Cs_2CO_3, DMF; (b) $SnCl_2·H_2O$, EtOAc; (c) (i) triphosgene, $NaHCO_3$, CH_2Cl_2, 0 °C; (ii) benzylamine derivatives, CH_2Cl_2, 0 °C; (d) boronic acid pinacol ester, $Ph(PPh_3)_4$, K_2CO_3, dioxane/H_2O (4:1), 95 °C.

nitrobenzene derivative **16**, followed by reduction of the nitro group using hydrated $SnCl_2$ to give aniline **17**. Treatment of **17** with triphosgene furnished an intermediate isocyanoaryl that was followed in one pot (without any workup) by a coupling reaction with an N-substituted benzylamine derivative to afford the bromide intermediate **18**. Finally, the target inhibitor **19** was formed via a palladium-catalyzed Suzuki reaction and was purified by reverse-phase preparative HPLC.

RESULTS AND DISCUSSION

The goal of this work was to develop potent and selective urea-based ROCK inhibitors possessing appropriate DMPK properties that would make them suitable for various potential applications by targeting the ROCK pathway. To do this, we evaluated these compounds in biochemical ROCK-II and protein kinase A (PKA) assays (PKA was selected as a routine counterscreen to gauge the general kinase selectivity of synthesized ROCK inhibitors[22−31]), and a few selected inhibitors were further assessed in JNK3, MRCKα, p38, and ROCK-I enzyme assays to screen for selectivity. After this, potent and selective inhibitors were submitted to cell-based assays that measured MLC bis-phosphorylation (ppMLC).[32] Finally, the most advanced ROCK-II inhibitors were evaluated in in vitro and in vivo DMPK studies.

Previously we reported that the aniline−benzylamine asymmetric urea coupled with an appropriate heteroaromatic hinge binding moiety was a good scaffold for ROCK inhibition.[22] For example, compound **5b** (Table 1), an unsubstituted urea-based ROCK-II inhibitor, showed good enzymatic and cellular potency and ∼32-fold selectivity against PKA (IC_{50} = 18 nM, 113 nM, and 586 nM, respectively).[22] To improve upon that, a variety of structural moieties other than benzylamines were applied to explore the structural elements that could fit well into the hydrophobic pocket (Figure 1). The distance between the urea carbonyl group and the terminal phenyl ring was first studied. Compounds **5a** to **5d** (corresponding to one to four backbone atoms between the carbonyl and the phenyl ring) were thus synthesized and evaluated. As shown in Table 1, the benzylamine-based urea **5b** is the most potent ROCK inhibitor. Replacement of the benzylamine by aniline (**5a**) significantly reduced the ROCK inhibition. Increasing the chain length from one methylene to two (**5c**) slightly decreased the potency while dramatic reduction of ROCK activity was observed when the chain length was increased to three methylene units (**5d**). Interestingly, the PKA selectivity did not change much with the chain length (∼30-fold) except for the aniline-based urea **5a** (>60-fold). These data suggest that changing the chain length between the urea moiety and the phenyl ring disturbed the optimal orientation of the phenyl group assumed in **5b**. It is important to note that the ring closure analogue of **5b** (**5h**, a bicyclic tetrahydroisoquinoline-based urea derivative) reduced potency of ROCK inhibition (IC_{50} = 280 nM). This lower potency of **5h** is in contrast to the potent ROCK inhibition (similar to **5b**) exhibited by its corresponding bicyclic carboxyl amide analogues developed in our lab (the tetrahydronaphthalene 2-carboxyl amide,[24] the chroman 3-carboxamide,[24] the benzadioxane 2-carboxamide,[23] and the tetrahydroisoquinoline 3-carboxamide[27]). The most likely reason for the lower ROCK

Table 1. SAR Studies for the Tail Moiety

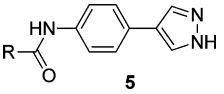

cmpd	R	ROCK-II[a] (nM)	ppMLC[a] (nM)	PKA[a] (nM)
5a	PhNH	304	n.d[b]	>20000
5b[c]	$PhCH_2NH$	18	113	586
5c	$PhCH_2CH_2NH$	88	>2700	3098
5d	$PhCH_2CH_2CH_2NH$	1017	n.d[b]	>20000
5e	$PhCH_2O$	7	>2700	>20000
5f	$PhCH_2CH_2O$	55	2635	>20000
5g	$PhCH_2CH_2$	24	91	266
5h	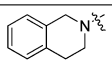	280	n.d[b]	8000
5i	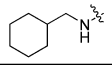	751	n.d[b]	>20000

[a]IC_{50} values are means of two or more experiments with errors within 30% of the mean. [b]Not determined. [c]Published results.[22]

dx.doi.org/10.1021/jm400062r | J. Med. Chem. XXXX, XXX, XXX−XXX

potency of **5h** was that the conformation assumed by the tetrahydroisoquinoline phenyl moiety was not as favored for hydrophobic interactions with the P-loop pocket as those in the carboxyl amide systems.

We next explored the feasibility of replacing the benzylamine with a benzyl alcohol or a phenylpropyl group while still maintaining potent ROCK inhibition. Table 1 shows the benzyl alcohol-derived analogue carbamate **5e** had a slightly improved ROCK potency (7 nM vs 18 nM) and a much better PKA selectivity (>300-fold vs 33-fold) as compared to urea **5b**. However, **5e** had lower cell activity (IC_{50} > 2700 nM). Just like in the urea series **5a–d**, addition of a methylene unit to the carbamate (**5f**) reduced ROCK inhibition. Although the corresponding carboxyl amide analogue **5g** presented ROCK inhibition similar to that of **5b**, its PKA selectivity was lower (~11-fold). On the other hand, **5g** exhibited good cell potency with an IC_{50} = 91 nM in the ppMLC assays (Table 1). In compound **5i**, a saturated cyclohexyl group was used to replace the aromatic phenyl ring in **5b**. As shown in Table 1, **5i** was a much weaker ROCK inhibitor than **5b** (IC_{50}: 751 nM vs 18 nM), which was likely due to a much weaker hydrophobic interaction with the P-loop for the cyclohexyl ring in **5i** than for the phenyl group in **5b**. The lower affinity for **5i** also demonstrated that hydrophobic interactions with the P-loop were likely a key contributor to ROCK inhibition for these urea-based inhibitors (and for inhibitors based on many other scaffolds developed in our laboratories[22−31]). Overall, data in Table 1 demonstrated that the benzylamine based urea was the best in terms of ROCK inhibition, cell potency, and PKA selectivity.

The effect of multisubstitutions on the benzyl phenyl ring was studied next. It was disclosed in our previous communication[22] that a 3-methoxy group was the best substituent in monosubstituted (on the benzyl phenyl ring) urea-based ROCK inhibitors (**5j**, IC_{50} = 2 nM in enzyme assay, 4 nM in cell assay, and 882 nM in PKA enzyme assay, Table 2).

Table 2. Effects of Disubstitutions on the Benzyl Phenyl Ring

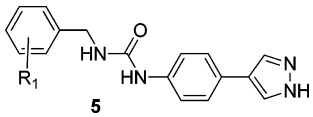

5

compd	R_1	ROCK-II[a] (nM)	PKA[a] (nM)
5j[b]	3-OCH_3	2	882
5k	2,3-di-OCH_3	253	>20000
5l	2,4-di-OCH_3	331	11170
5m	2,5-di-OCH_3	570	>20000
5n	2,6-di-OCH_3	924	13480
5o	3,4-di-OCH_3	425	>20000
5p	3,5-di-OCH_3	281	>20000
5q	3-F, 4-OCH_3	357	518

[a]IC_{50} values are means of two or more experiments with errors within 30% of the mean. [b]Published results.[22]

Several compounds with dimethoxy (**5k** to **5p**) or fluoro-methoxy (**5q**) substitutions were thus prepared and evaluated. As shown in Table 2, these compounds all possessed lower ROCK inhibition as compared to **5i**, regardless of the specific disubstitution pattern. One possible explanation for this observation is that these disubstitutions disturbed optimal hydrophobic interactions (exhibited in the monosubstituted inhibitor **5i**) between the phenyl moiety and the hydrophobic pocket under the P-loop. Alternatively, it is possible that the disubstitutions could not be accommodated in the pocket due to steric bulk.

The effect of substitutions on the urea NH group from the aniline side was the next focus of SAR studies. As shown in Table 3, any substitution to this position greatly reduced the

Table 3. Effects of Substitutions to the Urea NH of Aniline

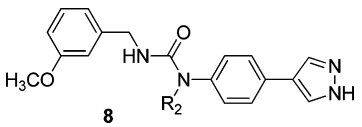

8

cmpd	R_2	ROCK-II[a] (nM)	PKA[a] (nM)
8a	-CH_3	87	>20000
8b	-CH_2CH_2OH	611	>20000
8c		2984	4196
8d	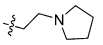	>20000	>20000
8e		3324	12010

[a]IC_{50} values are means of two or more experiments with errors within 30% of the mean.

ROCK affinity, and the deterioration of ROCK activity was in direct relation to the size of the substituents. For example, a simple methyl substitution resulted in compound **8a** which had moderate ROCK potency (IC_{50} = 87 nM, vs 2 nM in **5j**), while large substituents represented by compounds **8c–e** had ROCK IC_{50} values in the micromolar range. The major reason for the decreased ROCK potency was that substitution on this urea NH significantly disturbed the optimal binding conformation (see Figure 4, docking mode). Therefore, it was decided that no substitutions to this urea NH group would be made in future optimizations.

The effect of alkylation on the urea NH from the benzylamine side was previously communicated,[22] and results showed that this position was quite tolerant to simple methyl and ethyl groups. A more detailed set of SAR studies for substitutions on this position is summarized in Table 4. As expected, simple alkylation using methyl, ethyl, cyclopropyl, and isopropyl groups (**12a** to **12d**) furnished ROCK inhibitors exhibiting high potency in both enzyme and ppMLC cell assays and high selectivity against PKA (>1000-fold). Substitutions with oxygen-containing building blocks such as 2-hydroxylethyl and 2-methoxylethyl (**12e** and **12f**) also exhibited excellent enzymatic potency (IC_{50} was 1 nM and 17 nM, respectively), good to fair cellular activity (19 nM and 180 nM, respectively), and low PKA inhibition (2988 nM and 10530 nM, respectively). Interestingly, the compound containing a free NH_2 group (**12g**) exhibited modestly potent PKA inhibition (72 nM) in addition to high ROCK potency in both enzyme and cell-based assays (<1 nM and 8 nM, respectively). Remarkably, dimethylation of the NH_2 in **12g** resulted in an inhibitor (**12h**) with much lower PKA inhibition (456 nM) while still retaining excellent ROCK potency (IC_{50} < 1 and <4 nM in enzyme and cellular assay, respectively). Encouraged by **12h**, substitutions containing other tertiary amino alkyl groups (inhibitors **12i–n**) were prepared and evaluated. Like **12h**, these inhibitors had excellent ROCK potency and good to fair

dx.doi.org/10.1021/jm400062r | J. Med. Chem. XXXX, XXX, XXX–XXX

Table 4. Inhibitory and Metabolic Stability of Inhibitors 12 with Substitutions on Nitrogen of Benzylamine Moiety

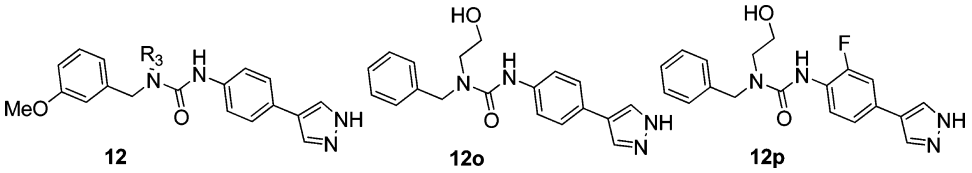

cmpd	R_3	ROCK-II[a] (nM)	ppMLC[a] (nM)	PKA[a] (nM)	HLM $t_{1/2}$ (min)
12a	-CH_3	1	4	1809	23
12b	-CH_2CH_3	1	44	4667	25
12c	-Cyclopropyl	1	4	1705	25
12d	-Isopropyl	3	67	18450	11
12e	-CH_2CH_2OH	1	19	2988	24
12f	-$CH_2CH_2OCH_3$	17	180	10530	21
12g	-$CH_2CH_2NH_2$	<1	8	72	>120
12h	-$CH_2CH_2N(CH_3)_2$	1	4	456	34
12i	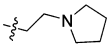	3	6	541	25
12j	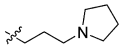	5	18	228	59
12k	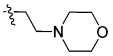	13	138	3823	3
12l	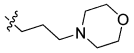	4	84	724	4
12m	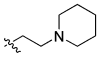	5	17	338	11
12n	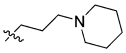	4	75	822	14
12o	-CH_2CH_2OH	12	59	610	>120
12p	-CH_2CH_2OH	14	33	1016	>120

[a]IC_{50} values were means of two or more experiments with errors within 30% of the mean.

Table 5. SAR of Substitutions on the α-Position of Benzylamine

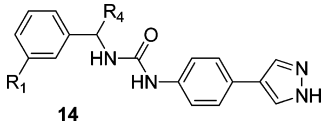

14

compd	R_1	R_4	ROCK-II[a] (nM)	ppMLC[a] (nM)	PKA[a] (nM)	HLM $t_{1/2}$ (min)
5j	OCH_3	H	2	4	882	34
14a	OCH_3	CH_2CH_2OH	2	40	4871	112
14b	F	CH_2CH_2OH	2	32	580	>120
14c	H	CH_2CH_2OH	1	48	438	>120
14d	H	CH_2OH	2	150	389	>120
14e	H	$CH_2CH_2N(CH_3)_2$	2	40	238	>60

[a]IC_{50} values are means of two or more experiments with errors within 30% of the mean.

cell activity and PKA selectivity. The only exception was **12j** which exhibited a PKA selectivity of only 25-fold.

The stability of these compounds in human liver microsomes (HLM) was also evaluated. Briefly, the microsomal stability of most inhibitors with simple alkyl or oxygen-containing alkyl substitutions (**12a** to **12f**) was good with the exception of the isopropyl-substituted compound **12d** (half-life was only 11 min). While the stability of compounds with substitutions containing NH_2, dimethylamino-, or pyrrolidino- (**12g** to **12j**) groups were good to excellent, inhibitors with substituents containing six-membered piperidine or morpholine moieties (**12k**–**n**) exhibited poor microsomal stability. The 3-methoxy substitution on the benzyl phenyl ring was clearly a liability for metabolic stability. For example, inhibitor **12e** exhibited a human microsomal stability of $t_{1/2}$ = 24 min, while the corresponding inhibitors without the methoxy substitution (**12o** and **12p**) had a much higher HLM stability of $t_{1/2}$ > 120 min. However, as shown in Table 4, the *m*-methoxy substitution benefited both the ROCK potency and the PKA selectivity.

The α-position of the benzylamine moiety is also an important point for diversification to fine-tune the pharmaceutical properties of this urea-based scaffold. Thus, ROCK inhibitors containing α-substitutions such as 2-hydroxyethyl, dimethylaminoethyl, and hydroxymethyl were synthesized and assessed (Table 5). Substitution of a 2-hydroxylethyl group to

dx.doi.org/10.1021/jm400062r | J. Med. Chem. XXXX, XXX, XXX–XXX

the α-position of **5j** resulted in inhibitor **14a** which showed equal biochemical potency and a much improved PKA selectivity (2 nM and 4871 nM, respectively) compared to **5j**. However, the cellular activity of **14a** (IC_{50} = 40 nM) was deteriorated and was probably due to the free OH group introduced with this substitution. Replacing the methoxy group in **14a** with a fluoride or hydrogen resulted in inhibitors (**14b** and **14c**) having similar biochemical and cellular potency but higher PKA inhibition (580 and 438 nM vs 4871 nM in **14a**). Similar enzyme and cellular potency was also observed for inhibitor **14e** which contained a dimethylaminoethyl substitution. Interestingly, shortening the chain length of the substitution in **14a** by one methylene unit (**14d**) did not affect the enzyme activity (ROCK-II and PKA) but led to slightly lower cellular potency (Table 5). Remarkably, introduction of a substitution to the benzyl α-position yielded ROCK inhibitors all possessing much higher microsomal stability (**14a** to **14e** vs **5j**). Overall, substitution on the α-position of the benzylamine moiety furnished ROCK inhibitors with excellent potency (both enzyme and cell), good PKA selectivity, and much improved microsomal stability (in contrast to substitutions on the urea NH group, Table 4, and substitutions on the middle phenyl ring[22]). Therefore, this type of ROCK inhibitor will be the focus for future optimizations.

In our previous communication,[22] simultaneous substitutions to both the middle phenyl ring with a large linear alkoxy group and the urea NH (from the benzylamine side) with a small methyl or ethyl group were well tolerated. This bis-substitution also improved the cell potency, the kinase selectivity, and the aqueous solubility. These beneficial effects were further confirmed in inhibitors with other bis-substitution combinations. For example, compound **19a** had a pyrrolidine-alkoxy group on the middle phenyl ring and an ethyl substituent on the urea NH (Figure 2). Compound **19b** possessed a

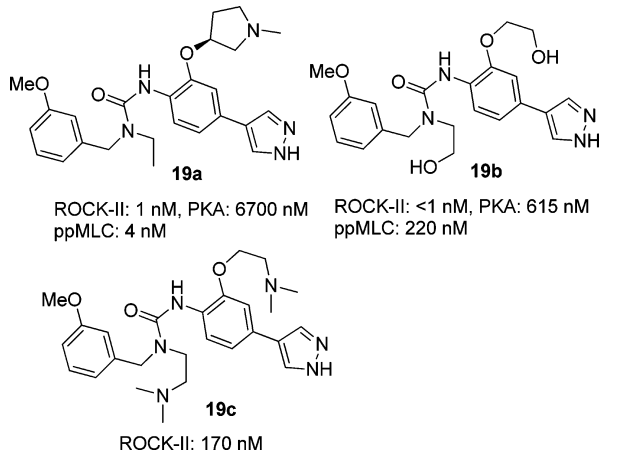

Figure 2. Substitution effects on both the middle phenyl ring and the urea NH of the benzylamine side. Simultaneous substitution by tertiary containing groups were not tolerated as demonstrated by compound **19c**.

hydroxyethyl substitution on both the middle phenyl ring and the urea NH (Figure 2). Although large, linear tertiary amine-containing substitutions on the urea NH were also well tolerated as demonstrated by compounds in Table 4, simultaneous bis-substitution of these two positions with two large groups (each containing a tertiary amine) was found to lessen ROCK inhibition. For example, compound **19c** in Figure 2 had a ROCK-II IC_{50} value which was >170-fold worse than that of the corresponding monosubstituted counterparts (**12h** in Table 4 and compound **1r** in ref 27).

For the middle phenyl ring of this urea scaffold, introduction of substituents containing a tertiary amino group improved ROCK potency, increased kinase selectivity, and enhanced aqueous solubility.[22] In the current study we found that replacement of the middle phenyl ring by a heteroaromatic moiety was also an important diversification strategy. For instance, a 2-yl-pyridine was used as a surrogate for the unsubstituted phenyl ring in compound **12h** to give **20** (Figure 3). This ROCK inhibitor (**20**) was highly potent (both enzyme

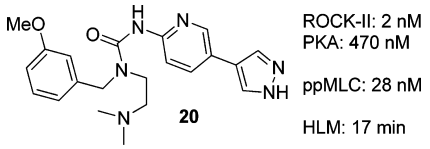

Figure 3. Replacement of the middle phenyl ring by a pyridine moiety was tolerated, presenting highly potent ROCK inhibitors.

and cell based) and had PKA selectivity similar to that of its counterpart analogue **12h** (Table 4). On the other hand, the introduction of the pyridine ring reduced HLM stability (from a half-life of 34 min in **12h** to a half-life of 17 min in **20**).

Molecular modeling was used to guide and explain the SAR and the optimizations for this urea-based scaffold. Several inhibitors were docked into the catalytic domain of a homology model of human ROCK-II enzyme developed by the methods previously described.[22−24,27] As shown in Figure 4A, the binding motif of compound **12e** revealed two H-bond interactions between residues Glu170/Met172 and the pyrazole group in the hinge region. A third H-bond interaction was formed between the urea N−H and the carbonyl group of the DFG domain residue Asp232. A fourth H-bond was formed between the OH moiety in the side chain of **12e** and the backbone carboxyl group of Asn219. In addition to H-bonding interactions, an important contributor to the high potency of **12e** was the hydrophobic interaction between the benzyl moiety of ligand and the enzyme hydrophobic pocket under the P-loop (Figure 4B). Similar docking modes were also observed for those α-position-substituted ROCK inhibitors listed in Table 5. As demonstrated by the binding motif of **14a** shown in Figure 4C, the OH moiety from the α-substituted side chain bound in the same direction as that in **12e** and formed an H-bond with residue Asn219 (not shown in figure).

The obtained structures of ligands bound to ROCK-II in the ATP-binding pocket explained the observed SAR quite well. To help analyze the SAR, a surface view for the binding mode of **12e** was presented in Figure 4B, which clearly showed areas on the inhibitor that could accommodate/tolerate substitutions. On the basis of these observations, it appeared that there was not enough space around the urea NH of the aniline side to accommodate a large substitution. Therefore, a small alkyl group such as a methyl (**8a**, Table 3) was tolerated and exhibited moderate ROCK inhibition, while a large substitution like those in **8b** to **8e** significantly deteriorated the ROCK affinity. Indeed, a large substitution at this position totally changed the binding motif as shown by that of **8c** in Figure 4D. The benzyl phenyl moiety in this inhibitor did not bind toward the P-loop, thus losing important hydrophobic interactions which were critical for effective ROCK inhibition. These modes

dx.doi.org/10.1021/jm400062r | J. Med. Chem. XXXX, XXX, XXX−XXX

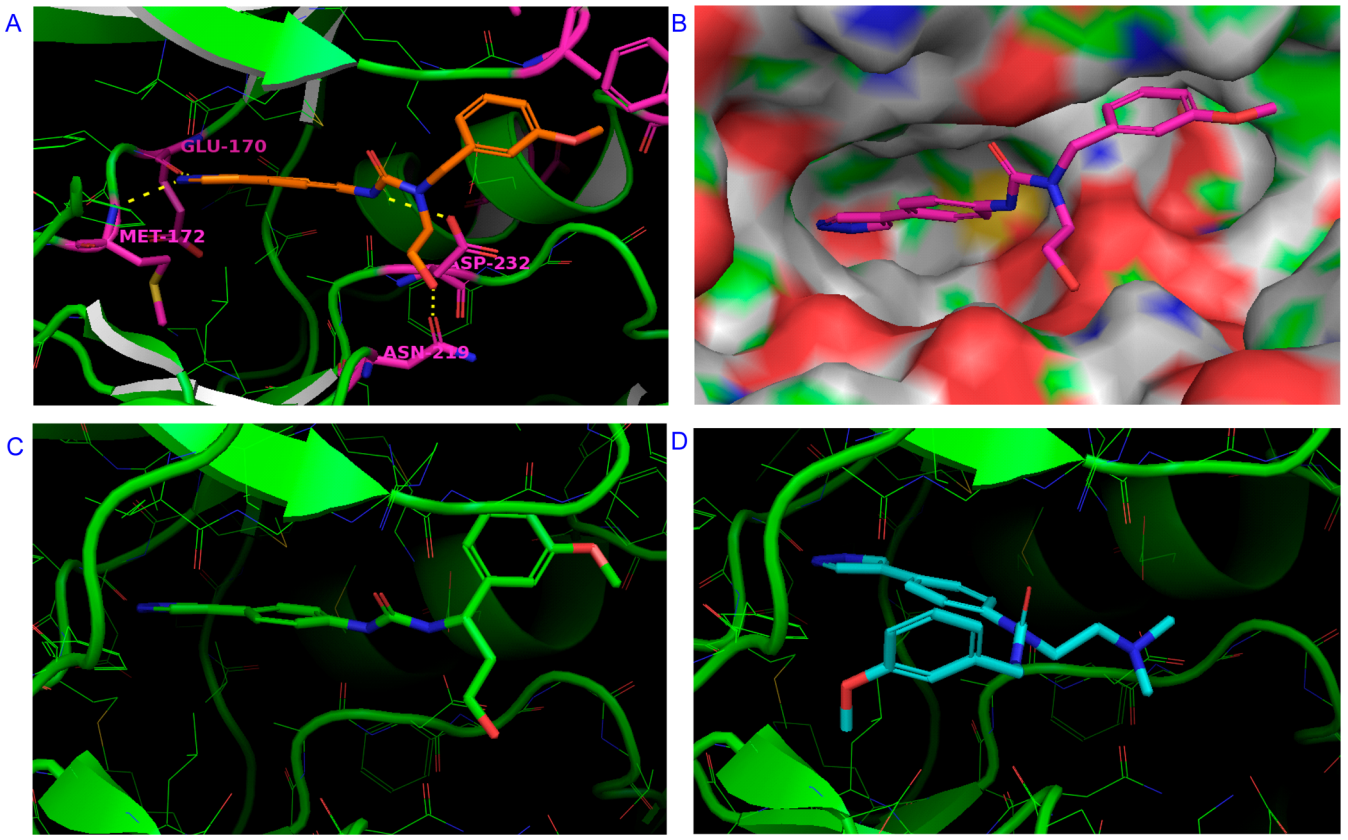

Figure 4. Docking modes of representative ROCK inhibitors bound to the ATP binding pocket of a homology model of human ROCK-II. A: **12e** with key H-bond interactions; B: the surface view for the mode of **12e**; C: the binding motif **14a** in ROCK-II which is very similar to that of **12e**; D: the binding motif **8c** in ROCK-II, which shows that the benzyl aromatic moiety is not interacted to the P-loop, thus resulting low ROCK potency.

could also explain the deteriorated ROCK activity of **5c**, **5d**, **5h**, **5i** (Table 1), and **5k** to **5q** (Table 2) as compared to that of **5b** and **5j**. Basically, the non-benzylamine structures (in Table 1) or the disubstituted benzylamine structures (in Table 2) had disturbed the optimal hydrophobic interactions between the benzyl phenyl moiety and the hydrophobic pocket under the P-loop. Finally, the surface view shown in Figure 4B clearly demonstrated that large substitutions could be well tolerated on the α-position of the benzyl moiety, on the urea NH of the benzylamine side, and on the 2′-position of the middle phenyl ring.

To evaluate the general selectivity of these urea-based ROCK inhibitors, some selected compounds were subjected to additional counter screening against ROCK-I, MRCKα, JNK3, and p38α in addition to PKA. These results are outlined in Table 6, and they demonstrate that these compounds had activity against MRCKα, the most closely related kinase to ROCK in the micromolar range and had no inhibition on JNK3 and p38α at concentrations >20 μM. Screening against ROCK-I showed that they were typically pan-ROCK inhibitors with potent ROCK-I inhibition. Inhibition of four selected purified cytochrome P450 isoforms (1A2, 2C9, 2D6, and 3A4) was tested at 10 μM and also demonstrated that these urea-based ROCK inhibitors had generally low inhibition for CYP1A2 and the most important CYP3A4 isoform. Given the low nanomolar ROCK potency of these compounds the relatively high % inhibition for some compounds seen at 10 μM for CYP2C9 and CYP2D6 was not viewed as overly concerning but will be the focus of further optimizations in this class.

Table 6. Inhibition over Chosen Kinases and P450 Enzymes

compd	MRCKα[a] IC_{50} (nM)	JNK[a] IC_{50} (μM)	p38α[a] IC_{50} (μM)	ROCK-I[a] IC_{50} (nM)	1A2/2C9/2D6/3A4% inhib at 10 μM
12a	1853	>20	>20	4	9/96/45/27[b]
12e	4306	>20	>20	6	−23/95/38/37[b]
12h	8695	>20	>20	6	−29/35/85/34[b]
12i	n.d[c]	>20	>20	13	0/24/88/34
12k	n.d[c]	>20	>20	58	−37/68/82/51
12m	n.d[c]	>20	>20	14	18/56/87/61
12o	n.d[c]	n.d[c]	n.d[c]	33	9/93/29/15
14a	n.d[c]	n.d[c]	n.d[c]	11	3/67/37/37
14b	6400	>20	>20	10	−2/71/41/23
14e	n.d[c]	n.d[c]	n.d[c]	6	−1/16/59/10
19a	1550	>20	>20	4	9/65/83/53
20	n.d[c]	n.d[c]	n.d[c]	10	−21/5/51/8

[a]Data were averaged from two or more measurements with errors within 30% of the average. [b]IC_{50}s (μM) of 1A2/2C9/3D6/3A4: >100/0.6/>100/>100 for **12a**; >100/2/40/35 for **12e**; >100/30/3/80 for **12h**. [c]Not determined.

Several inhibitors were also evaluated in rats in vivo to determine pharmacokinetic properties (Table 7). In summary, ROCK inhibitors with a simple alkyl substitution or a substitution containing a hydroxyl group normally exhibited low clearance and low volume of distribution, high AUC and C_{max}, and good oral bioavailability (**12a**, **12b**, **12o**, and **14b**). On the other hand, compounds containing an amino moiety generally had high clearance and high volume of distribution, low AUC and C_{max}, and zero to very low oral bioavailability

dx.doi.org/10.1021/jm400062r | J. Med. Chem. XXXX, XXX, XXX−XXX

Table 7. In Vivo PK Data in Rats[a]

compd	Cl (iv)[b] (mL/min/kg)	V_d (iv)[b] (L/kg)	$T_{1/2}$ (iv)[b] (h)	AUC (iv)[b] (μM·h)	C_{max} (iv)[b] (μM)	% F,[c] po
12a	9.4	1.1	1.0	5.9	2.6	48
12e	11.2	1.0	1.6	4.2	3.8	51
12h	176	14	1.0	0.2	0.33	10
12i	71	4.4	1.0	0.6	0.48	0
12k	63	3.5	2.2	0.6	1.2	4
12m	86	4.3	1.0	0.4	0.53	0
12o	31	1.9	1.9	3.6	1.1	46
14a	5.9	0.25	0.7	7.9	12	4
14b	4.9	0.7	2.1	9.5	9.2	28
14e	91	20	2.4	0.5	0.2	0
19a	30	2.6	1.0	1.3	1.1	11

[a]Data reported were the mean of three determinations, and the standard error is within 40% of the mean. [b]iv, 1 mg/kg. [c]po, 2 mg/kg.

(**12h**, **12i**, **12k**, **12m**, and **14a**). The low oral bioavailability property of the amino group containing ROCK inhibitors was probably due to the protonation of the amino group under the physiological environment.

CONCLUSION

The detailed SAR studies (presented here and in our previous communication[22]) demonstrated that urea structures derived from anilines and benzylamines are very good for ROCK inhibition. More importantly, this urea scaffold can provide multipoint diversification which could be applied to manipulate the inhibitor's pharmaceutical properties such as selectivity, solubility, and in vitro and in vivo DMPK properties. Through our SAR studies, good ROCK inhibitors with various DMPK properties suitable for different applications were discovered. Basically, these lead compounds can be grouped into two classes. One class of compounds are those ROCK inhibitors that possess good in vivo PK properties (systemic) such as compounds **12a**, **12e**, **12o**, and **14b** in Table 7. A common feature of these compounds is that they do not have a tertiary amino moiety on their side chains. These compounds could serve as good candidates for systemic applications such as for the treatment of MS, cardiovascular diseases, ED, pain, etc. The second class of compounds are those ROCK inhibitors that have poor (systemic) PK properties such as compounds **12h**, **12i**, **12k**, **12m**,**14a**, **14e**, and **19a** in Table 7 (and **20**). These compounds all possess a tertiary amine group on their side chains and generally have good aqueous solubility. This class of compounds is good for topical applications such as in the treatment of glaucoma, ED, and pulmonary hypertension, etc.

In our previous communication, the optimization focused more on substitutions to the central phenyl ring.[22] These compounds generally exhibited poor systemic PK properties mainly due to destruction to the symmetry of the central phenyl ring.[33] Therefore, they are basically more suitable for topical applications. In the full SAR studies described in this manuscript, potent ROCK inhibitors possessing good in vivo systemic PK properties have been discovered, and they are mainly derived from those compounds without a large substitution on their central phenyl ring.

EXPERIMENTAL SECTION

Commercially available reagents and anhydrous solvents were used without further purification unless otherwise specified. Thin layer chromatography (TLC) analyses were performed with precoated silica gel 60 F254. The mass spectra were recorded by LC/MS with Finnigan LCQ Advantage MAX spectrometer of Thermo Electron. Flash chromatography was performed on prepacked columns of silica gel (230−400 mesh, 40−63 μm) by CombiFlash with EtOAc/hexane or MeOH/DCM as eluents. The preparative HPLC was performed on SunFire C_{18} OBD 10 μm (30 × 250 mm) with CH_3CN + 50% MeOH/H_2O + 0.1% TFA as eluents to purify the targeted compounds. Analytic HPLC was performed on Agilent technologies 1200 series with CH_3CN (Solvent B)/H_2O + 0.9% CH_3CN + 0.1% TFA (Solvent A) as eluents, and the targeted products were detected by UV in the detection range of 215−310 nm. All compounds were determined to be >95% pure by this method. NMR spectra were recorded with a Bruker 400 MHz spectrometer at ambient temperature with the residual solvent peaks as internal standards. The line positions of multiplets were given in ppm (δ) and the coupling constants (J) were given in hertz. The high-resolution mass spectra (HRMS, electrospray ionization) experiments were performed with Thermo Finnigan orbitrap mass analyzer. Data were acquired in the positive ion mode at resolving power of 100 000 at m/z 400. Calibration was performed with an external calibration mixture immediately prior to analysis.

General Synthetic Procedures. A primary amine or alcohol (0.2 mmol) was added to a solution of 1-bromo-4-isocyanatobenzene (**2**, 0.2 mmol) in DCM (1 mL). The mixture was stirred at room temperature until **2** was completely conversed. Then the solvent was removed in vacuo to obtain the crude urea or carbamate intermediate **4**. In an alternative route, 4-bromoaniline (**3**, 0.2 mmol) was added to a mixture of 3-phenylpropanoic acid (0.2 mmol), HATU (0.2 mmol), and DIEA (0.6 mmol) in DMF. The mixture was stirred at room temperature until **3** was completely conversed. Then the reaction was quenched by saturated $NaHCO_3$ and extracted with ethyl acetate (3 × 5 mL). The combined organic layers were dried over anhydrous Na_2SO_4 and concentrated in vacuo to give the crude carboxamide intermediate **4**.

1-(Isocyanomethyl)-3-methoxybenzene (0.2 mmol) was added to a solution of N-substituted 4-bromoaniline **6** (0.2 mmol) in DCM (1 mL). The mixture was stirred at room temperature until **6** was totally converted. Then the solvent was removed in vacuo to obtain the crude bromide intermediate **7**.

To a solution of 3-substituted aldehyde (**9**, 10 mmol) in methanol (20 mL) was added a primary amine (10 mmol). After being stirred at room temperature for 15 min, the solution was cooled to 0 °C prior to the addition of sodium borohydride (5 mmol) portionwise. The resulting solution was stirred at room temperature for 1 h. After the addition of water (3 mL), methanol was removed under reduced pressure and the resulting aqueous phase was extracted with EtOAc (3 × 15 mL). The combined extracts were dried over anhydrous Na_2SO_4 and concentrated in vacuo to give the secondary benzylamine. Then secondary benzylamine (0.2 mmol) was then added to a mixture of 1-bromo-4-isocyanatobenzene (**2**, 0.2 mmol) in DCM at 0 °C. After being stirred at room temperature for 0.5−12 h, the mixture was extracted with DCM (3 × 5 mL), dried over anhydrous Na_2SO_4, and concentrated in vacuo to give the crude bromide intermediate **11** which was used in the next step without further purification.

α-Substituted benzylamine (0.2 mmol) was added to a solution of 1-bromo-4-isocyanatobenzene (**2**, 0.2 mmol) in DCM (1 mL). The mixture was stirred at room temperature until **2** was completely conversed. Then the solvent was removed in vacuo to obtain the crude intermediate **13**.

To a mixture of 4-bromo-2-fluoro-nitrobenzene (**15**, 1 mmol) and Cs_2CO_3 (3 mmol) in DMF (5 mL) was added *N*, *N*-dimethylaminoethanol or methanol (1.05 mmol). After the complete conversion of the starting material detected by TLC, the mixture was quenched by water (2 mL) and extracted with EtOAc (3 × 5 mL). The combined organic extracts were washed with saturated brine, dried over anhydrous Na_2SO_4, concentrated under reduced pressure, and purified through silica gel to give **16**. To a solution of **16** (1 mmol) in EtOAc (5 mL) was added tin chloride dihydrate (3 mmol). The stirring was continued at room temperature until the complete disappearance of **16** as detected by LC/MS, and the mixture was then

dx.doi.org/10.1021/jm400062r | J. Med. Chem. XXXX, XXX, XXX−XXX

quenched by water (2 mL) and extracted with EtOAc (3 × 5 mL). The combined organic extracts were washed with saturated brine, dried over anhydrous Na_2SO_4, concentrated under reduced pressure, and purified through silica gel to give aniline **17**. Triphosgene (0.07 mmol) was added to a mixture of **17** (0.2 mmol) and saturated $NaHCO_3$ (0.5 mL) in DCM (1 mL) at 0 °C to produce the isocyano intermediate. Then N^1-(3-methoxybenzyl)-N^2,N^2-dimethylethane-1,2-diamine (0.2 mmol) in DCM (1 mL) was added to the mixture of isocyano intermediate at 0 °C. After being stirred at room temperature for 0.5 h, the mixture was extracted with DCM (3 × 5 mL), dried over anhydrous Na_2SO_4, and concentrated in vacuo to give the crude bromide intermediate **18** which was used in the next step without further purification.

Finally, the 1*H*-pyrazoleboronic acid pinacol ester (0.3 mmol) and the crude intermediates **4**, **7**, **11**, **13**, and **18** (0.2 mmol) were dissolved in degassed 5:1 dioxane/H_2O. $Pd(PPh_3)_4$ (0.02 mmol) and a 2 M solution of K_2CO_3 (0.6 mmol) were added sequentially under argon, and the mixture was heated at 95 °C for 2 h. After being cooled to room temperature, the mixture was diluted with water and extracted with ethyl acetate (3 × 5 mL). The organic layers were combined, dried over anhydrous Na_2SO_4, and concentrated in vacuo. The residue was then subjected to preparative HPLC to give the target products **5**, **8**, **12**, **14**, **19**, and **20** as a white powder.

*1-(4-(1H-Pyrazol-4-yl)phenyl)-3-phenylurea (**5a**).* 56% yield in two steps. ^{1}H NMR (DMSO-d_6, 400 MHz) δ 12.85 (s, br, 1H), 8.64 (s, 1H), 8.09 (s, 1H), 7.85 (s, 1H), 7.52−7.42 (m, 6H), 7.29−7.25 (m, 2H), 6.98−6.94 (m, 1H); ^{13}C NMR (DMSO-d_6, 100 MHz) δ 152.51, 139.73, 137.63, 135.96, 128.74, 126.65, 125.50, 124.86, 121.72, 121.03, 118.55, 118.13; LC/MS (M + H$^+$) 279. HRMS (ESI-Orbitrap) calcd for $C_{16}H_{15}N_4O$ [M + H$^+$]: 279.1246, found 279.1244.

*1-(4-(1H-Pyrazol-4-yl)phenyl)-3-benzylurea (**5b**).* 75% yield in two steps. ^{1}H NMR (DMSO-d_6, 400 MHz) δ 12.81 (br, s, 1H), 8.52 (s, 1H), 7.93 (s, 2H), 7.45 (dd, J = 6.8, 2.0 Hz, 2H), 7.38 (dd, J = 6.8, 2.0 Hz, 2H), 7.36−7.30 (m, 4H), 7.26−7.22 (m, 1H), 6.58 (t, J = 5.6 Hz, 1H), 4.30 (d, J = 5.6 Hz, 2H); ^{13}C NMR (DMSO-d_6, 100 MHz) δ 158.67, 155.19, 150.36, 140.35, 138.40, 128.27, 127.08, 126.67, 125.95, 125.41, 121.10, 118.07, 42.71; LC/MS (M + H$^+$): 293; HRMS (ESI-Orbitrap) calcd for $C_{17}H_{17}N_4O$: 293.1402 [M + H$^+$], found 293.1393.

*1-(4-(1H-Pyrazol-4-yl)phenyl)-3-phenethylurea (**5c**).* 78% yield in two steps. ^{1}H NMR (DMSO-d_6, 400 MHz) δ 8.45 (s, 1H), 7.93 (s, 2H), 7.44 (d, J = 8.4 Hz, 2H), 7.35 (d, J = 8.4 Hz, 2H), 7.30 (d, J = 8.0 Hz, 2H), 7.25 (d, J = 8.0 Hz, 2H), 7.21−7.20 (m, 1H), 6.08 (t, J = 5.6 Hz, 1H), 3.35 (dt, J = 6.8, 5.6 Hz, 2H), 2.75 (t, J = 6.8 Hz, 2H); ^{13}C NMR (DMSO-d_6, 100 MHz) δ 155.13, 139.54, 138.52, 130.15, 129.86, 128.65, 128.33, 126.04, 125.81, 125.42, 121.17, 117.97, 40.60, 35.86; LC/MS (M + H$^+$): 307. HRMS (ESI-Orbitrap) calcd for $C_{18}H_{19}N_4O$: 307.1559 [M + H$^+$], found 307.1566.

*1-(4-(1H-Pyrazol-4-yl)phenyl)-3-(3-phenylpropyl)urea (**5d**).* 78% yield in two steps. ^{1}H NMR (DMSO-d_6, 400 MHz) δ 8.39 (s, 1H), 7.93 (s, 2H), 7.50 (d, J = 8.8 Hz, 2H), 7.36 (d, J = 8.8 Hz, 2H), 7.31−7.2 (m, 2H), 7.23−7.16 (m, 3H), 6.17 (t, J = 5.6 Hz, 1H), 3.12−3.07 (m, 2H), 2.63−2.59 (m, 2H), 1.77−1.70 (m, 2H); ^{13}C NMR (DMSO-d_6, 100 MHz) δ 156.20, 142.66, 139.54, 131.47, 130.89, 129.24, 129.23, 126.76, 126.67, 126.38, 122.19, 118.96, 39.63, 33.45, 32.54; LC/MS (M + H$^+$): 321. HRMS (ESI-Orbitrap) calcd for $C_{18}H_{19}N_4O$: 321.1715 [M + H$^+$], found 321.1722.

*Benzyl 4-(1H-pyrazol-4-yl)phenylcarbamate (**5e**).* 67% yield in two steps. ^{1}H NMR (DMSO-d_6, 400 MHz) δ 12.85 (s, br, 1H), 9.72 (s, 1H), 8.08 (s, 1H), 7.84 (s, 1H), 7.52−7.50 (m, 2H), 7.45−7.32 (m, 7H), 5.15 (s, 2H); 13C NMR (DMSO-d_6, 100 MHz) δ 153.32, 136.92, 136.64, 135.86, 128.42, 128.05, 127.99, 127.29, 125.45, 124.82, 120.89, 118.54, 65.66; LC/MS (M + H$^+$) 294. HRMS (ESI-Orbitrap) calcd for $C_{18}H_{18}N_3O$ [M + H$^+$]: 294.1243, found 294.1238.

*Phenethyl 4-(1H-pyrazol-4-yl)phenylcarbamate (**5f**).* 61% yield in two steps. ^{1}H NMR (DMSO-d_6, 400 MHz) δ 9.58 (s, br, 1H), 7.97 (s, 1H), 7.65−7.60 (m, 2H), 7.58−7.57 (m, 1H), 7.56−7.54 (m, 2H), 7.51−7.42 (m, 1H), 7.35−7.30 (m, 3H), 7.26−7.22 (m, 1H), 4.31 (t, J = 6.8 Hz, 2H), 2.96 (t, J = 6.8 Hz, 2H); ^{13}C NMR (DMSO-d_6, 100 MHz) δ 153.43, 138.08, 137.00, 132.15, 131.50, 128.83, 128.78, 128.67, 128.35, 126.31, 125.42, 118.59, 64.63, 34.72; LC/MS (M + H$^+$) 308; HRMS (ESI-Orbitrap) calcd for $C_{18}H_{18}N_3O$ [M + H$^+$]: 308.1399, found 308.1405.

*N-(4-(1H-Pyrazol-4-yl)phenyl)-3-phenylpropanamide (**5g**).* 75% yield in two steps. ^{1}H NMR (DMSO-d_6, 400 MHz) δ 12.86 (s, br, 1H), 9.88 (s, 1H), 8.10 (, 1H), 7.85 (s, 1H), 7.57−7.50 (m, 4H), 7.31−7.24 (m, 4H), 7.20−7.16 (m, 1H), 2.91 (t, J = 7.6 Hz, 2H), 2.62 (t, J = 7.6 Hz, 2H)); ^{13}C NMR (DMSO-d_6, 100 MHz) δ 170.16, 141.18, 137.14, 135.93, 135.67, 128.28, 128.21, 127.80, 125.90, 125.31, 120.92, 119.40, 37.92, 30.82; LC/MS (M + H$^+$) 292; HRMS (ESI-Orbitrap) calcd for $C_{18}H_{18}N_3O$ [M + H$^+$]: 292.1450, found 292.1451.

*1-(4-(1H-Pyrazol-4-yl)phenyl)-3-(cyclohexylmethyl)urea (**5i**).* 72% yield in two steps. ^{1}H NMR (DMSO-d_6, 400 MHz) δ 8.35 (s, 1H), 7.94 (s, 2H), 7.44 (d, J = 8.4 Hz, 2H), 7.35 (d, J = 8.4 Hz, 2H), 6.14−6.12 (m, 1H), 2.95−2.92 (m, 2H), 1.70−1.62 (m, 5H), 1.38−1.37 (m, 1H), 1.25−1.12 (m, 3H), 0.94−0.86 (m, 2H); ^{13}C NMR (DMSO-d_6, 100 MHz) δ 155.22, 138.60, 130.04, 125.67, 125.40, 121.15, 117.83, 111.63, 45.25, 37.96, 30.31, 26.06, 25.39; LC/MS (M + H$^+$) 299; HRMS (ESI-Orbitrap) calcd for $C_{19}H_{20}FN_4O_2$ [M + H$^+$]: 299.1872, found 299.1877.

*1-(4-(1H-Pyrazol-4-yl)phenyl)-3-(3-methoxybenzyl)urea (**5j**).* 86% yield in two steps. ^{1}H NMR (DMSO-d_6, 400 MHz) δ 8.52 (s, 1H), 7.94 (s, 2H), 7.45 (d, J = 8.8 Hz, 2H), 7.37 (d, J = 8.8 Hz, 2H), 7.25 (m, 1H), 6.87 (m, 2H), 6.80 (m, 1H), 6.57 (t, J = 5.6 Hz, 1H), 4.27 (d, J = 5.6 Hz, 2H), 3.74 (s, 3H); ^{13}C NMR (DMSO-d_6, 100 MHz) δ 159.30, 155.20, 142.00, 138.43, 137.56, 130.15, 129.34, 125.91, 125.42, 121.13, 119.22, 118.06, 112.76, 111.99, 54.95, 42.67; LC/MS (M + H$^+$): 323; HRMS (ESI-Orbitrap) calcd for $C_{18}H_{19}N_4O_2$ [M + H$^+$]: 323.1508, found 323.1496.

*1-(4-(1H-Pyrazol-4-yl)phenyl)-3-(2,3-dimethoxybenzyl)urea (**5k**).* 75% yield in two steps. ^{1}H NMR (DMSO-d_6, 400 MHz) δ 8.53 (s, 1H), 7.94 (s, 2H), 7.45 (d, J = 8.8 Hz, 2H), 7.36 (d, J = 8.8 Hz, 2H), 7.05−7.01 (m, 1H), 6.97−6.95 (m, 1H), 6.88−6.86 (m, 1H), 6.43 (t, J = 6.0 Hz, 1H), 4.28 (d, J = 6.0 Hz, 2H), 3.80 (s, 3H), 3.78 (s, 3H); ^{13}C NMR (DMSO-d_6, 100 MHz) δ 155.08, 154.37, 152.24, 146.23, 138.46, 133.42, 130.13, 125.84, 125.43, 123.80, 121.15, 120.16, 117.96, 111.73, 60.04, 55.65, 37.78; LC/MS (M + H$^+$): 353. HRMS (ESI-Orbitrap) calcd for $C_{18}H_{19}N_4O$ [M + H$^+$]: 353.1614, found 353.1620.

*1-(4-(1H-Pyrazol-4-yl)phenyl)-3-(2,4-dimethoxybenzyl)urea (**5l**).* 77% yield in two steps. ^{1}H NMR (DMSO-d_6, 400 MHz) δ 8.51 (s, 1H), 7.93 (s, 2H), 7.44 (dd, J = 6.8, 2.0 Hz, 2H), 7.35 (dd, J = 6.8, 2.0 Hz, 2H), 7.12 (d, J = 8.4 Hz, 1H), 6.56 (d, J = 2.4 Hz, 1H), 6.48 (dd, J = 8.4, 2.4 Hz, 1H), 6.31 (t, J = 5.6 Hz, 1H), 4.16 (d, J = 5.6 Hz, 2H), 3.81 (s, 3H), 3.74 (s, 3H); ^{13}C NMR (DMSO-d_6, 100 MHz) δ 159.72, 158.33, 157.81, 155.07, 138.52, 130.05, 129.02, 125.78, 125.43, 121.16, 119.82, 117.87, 104.22, 98.25, 55.39, 55.16, 37.84; LC/MS (M + H$^+$): 353. HRMS (ESI-Orbitrap) calcd for $C_{18}H_{19}N_4O$ [M + H$^+$]: 353.1614, found 353.1609.

*1-(4-(1H-Pyrazol-4-yl)phenyl)-3-(2,5-dimethoxybenzyl)urea (**5m**).* 69% yield in two steps. ^{1}H NMR (DMSO-d_6, 400 MHz) δ 12.81 (s, br, 1H), 8.57 (s, 1H), 8.05 (s, 1H), 7.82 (s, 1H), 7.44 (dd, J = 6.8, 2.0 Hz, 2H), 7.36 (dd, J = 6.8, 2.0 Hz, 2H), 6.92−6.90 (m, 1H), 6.82−6.78 (m, 2H), 6.41 (t, J = 6.0 Hz, 1H), 4.22 (d, J = 6.0 Hz, 2H), 3.77 (s, 3H), 3.68 (s, 3H); ^{13}C NMR (DMSO-d_6, 100 MHz) δ 155.13, 153.03, 150.84, 138.43, 128.89, 127.73, 125.92, 125.43, 121.15, 117.98, 114.64, 111.61, 111.35, 99.49, 55.74, 55.32, 38.16; LC/MS (M + H$^+$): 353. HRMS (ESI-Orbitrap) calcd for $C_{18}H_{19}N_4O$ [M + H$^+$]: 353.1614, found 353.1610.

*1-(4-(1H-Pyrazol-4-yl)phenyl)-3-(2,6-dimethoxybenzyl)urea (**5n**).* 67% yield in two steps. ^{1}H NMR (DMSO-d_6, 400 MHz) δ 8.44 (s, 1H), 7.93 (s, 2H), 7.43 (d, J = 8.8 Hz, 2H), 7.33 (d, J = 8.8 Hz, 2H), 7.26 (t, J = 8.4 Hz, 1H), 6.67 (d, J = 8.4 Hz, 2H), 6.01 (t, J = 5.2 Hz, 1H), 4.29 (d, J = 5.2 Hz, 2H), 3.81 (s, 6H); ^{13}C NMR (DMSO-d_6, 100 MHz) δ 158.10. 154.83, 138.58, 130.15, 129.87, 128.96, 125.70, 125.44, 121.20, 117.74, 114.23, 104.04, 55.81, 31.84; LC/MS (M + H$^+$): 353. HRMS (ESI-Orbitrap) calcd for $C_{18}H_{19}N_4O$ [M + H$^+$]: 353.1614, found 353.1608.

*1-(4-(1H-Pyrazol-4-yl)phenyl)-3-(3,4-dimethoxybenzyl)urea (**5o**).* 76% yield in two steps. ^{1}H NMR (DMSO-d_6, 400 MHz) δ 8.48 (s, 1H), 7.94 (s, 2H), 7.45 (d, J = 8.8 Hz, 2H), 7.37 (d, J = 8.8 Hz, 2H), 6.92−6.90 (m, 2H), 6.84−6.82 (m, 1H), 6.49 (t, J = 5.6 Hz, 1H), 4.21

dx.doi.org/10.1021/jm400062r | J. Med. Chem. XXXX, XXX, XXX−XXX

(d, J = 5.6 Hz, 2H), 3.74 (s, 3H), 3.72 (s, 3H); ^{13}C NMR (DMSO-d_6, 100 MHz) δ 155.14, 150.03, 148.64, 147.72, 138.46, 132.68, 130.26, 125.91, 125.42, 121.25, 119.26, 118.05, 111.78, 111.32, 55.55, 55.42, 42.57; LC/MS (M + H$^+$): 353. HRMS (ESI-Orbitrap) calcd for $C_{18}H_{19}N_4O$ [M + H$^+$]: 353.1614, found 353.1608.

1-(4-(1H-Pyrazol-4-yl)phenyl)-3-(3,5-dimethoxybenzyl)urea (**5p**). 79% yield in two steps. ^{1}H NMR (DMSO-d_6, 400 MHz) δ 12.82 (s, br, 1H), 8.53 (s, 1H), 7.96−7.94 (m, 2H), 7.45 (d, J = 8.8 Hz, 2H), 7.38 (d, J = 8.8 Hz, 2H), 6.56 (t, J = 5.6 Hz, 1H), 6.47−6.46 (m, 2H), 6.37 (s, 1H), 4.22 (d, J = 5.6 Hz, 2H), 3.72 (s, 6H); ^{13}C NMR (DMSO-d_6, 100 MHz) δ 160.47, 155.19, 142.80, 138.42, 134.32, 130.29, 125.96, 125.42, 118.07, 105.02, 98.77, 98.33, 55.08, 42.79; LC/MS (M + H$^+$): 353; HRMS (ESI-Orbitrap) calcd for $C_{18}H_{19}N_4O$ [M + H$^+$]: 353.1614, found 353.1611.

1-(4-(1H-Pyrazol-4-yl)phenyl)-3-(3-fluoro-4-methoxybenzyl)urea (**5q**). 76% yield in two steps. ^{1}H NMR (DMSO-d_6, 400 MHz) δ 12.82 (s, br. 1H), 8.53 (s, 1H), 8.06 (s, 1H), 7.82 (s, 1H), 7.45 (dd, J = 6.8, 2.0 Hz, 2H), 7.37 (dd, J = 6.8, 2.0 Hz, 2H), 7.15−7.06 (m, 3H), 6.57 (t, J = 6.0 Hz, 1H), 4.22 (d, J = 6.0 Hz, 2H), 3.81 (s, 3H); ^{13}C NMR (DMSO-d_6, 100 MHz) δ 155.17, 152.50, 150.07, 145.87, 138.37, 133.52, 125.98, 125.41, 123.24, 121.11, 118.11, 114.79, 114.61, 113.71, 55.99, 41.84; LC/MS (M + H$^+$): 341; HRMS (ESI-Orbitrap) calcd for $C_{18}H_{19}N_4O$ [M + H$^+$]: 341.1414, found 341.1412.

1-(4-(1H-Pyrazol-4-yl)phenyl)-3-(3-methoxybenzyl)-1-methylurea (**8a**). 82% yield in two steps. ^{1}H NMR (DMSO-d_6, 400 MHz) δ 8.06 (s, 2H), 7.62 (d, J = 6.8, 2.0 Hz, 2H), 7.26 (d, J = 6.8, 2.0 Hz, 2H), 7.22−7.18 (m, 1H), 6.82−6.75 (m, 3H), 6.48 (t, J = 5.6 Hz, 1H), 4.18 (d, J = 5.6 Hz, 2H), 3.73 (s, 3H), 3.17 (s, 3H); ^{13}C NMR (DMSO-d_6, 100 MHz) δ 159.15, 158.48, 156.80, 142.69, 141.66, 130.77, 130.61, 129.06, 126.98, 125.93, 120.69, 119.09, 112.55, 111.66, 54.86, 43.53, 37.05; LC/MS (M + H$^+$) 337; HRMS (ESI-Orbitrap) calcd for $C_{19}H_{21}N_4O_2$ [M + H$^+$]: 337.1665, found 337.1653.

1-(4-(1H-Pyrazol-4-yl)phenyl)-1-(2-hydroxyethyl)-3-(3-methoxybenzyl)urea (**8b**). 28% yield in four steps. ^{1}H NMR (DMSO-d_6, 400 MHz) δ 8.08 (s, 2H), 7.64 (d, J = 8.4 Hz, 2H), 7.26 (d, J = 8.4 Hz, 2H), 7.21−7.17 (m, 1H), 6.80−6.75 (m, 3H), 6.24 (t, J = 6.0 Hz, 1H), 4.16 (d, J = 6.0 Hz, 2H), 3.73 (s, 3H), 3.62 (t, J = 6.0 Hz, 2H), 3.46 (t, J = 6.0 Hz, 2H); ^{13}C NMR (DMSO-d_6, 100 MHz) δ 159.42, 159.13, 157.78, 156.83, 143.88, 142.71, 140.20, 131.40, 129.06, 128.61, 126.08, 118.98, 112.35, 111.70, 58.99, 54.85, 51.56, 43.45; LC/MS (M + 1) 367; HRMS (ESI-Orbitrap) calcd for $C_{20}H_{23}N_4O_3$ [M + H$^+$]: 367.1770, found 367.1758.

1-(4-(1H-Pyrazol-4-yl)phenyl)-1-(2-(dimethylamino)ethyl)-3-(3-methoxybenzyl)urea (**8c**). 26% yield in four steps. ^{1}H NMR (DMSO-d_6, 400 MHz) δ 9.33 (br, s, 1H), 8.11 (s, 2H), 7.71 (d, J = 8.4 Hz, 2H), 7.34 (d, J = 8.4 Hz, 2H), 7.36−7.17 (m, 1H), 6.79−6.76 (m, 3H), 6.43 (t, J = 6.0 Hz, 1H), 4.17 (d, J = 6.0 Hz, 2H), 3.92 (dd, J = 11.6, 6.4 Hz, 2H), 3.72 (s, 3H), 3.16 (dd, J = 11.6, 6.4 Hz, 2H), 2.84 (s, 3H), 2.83 (s, 3H); ^{13}C NMR (DMSO-d_6, 100 MHz) δ 159.14, 158.44, 157.68, 142.39, 138.49, 132.40, 129.08, 128.85, 126.50, 119.01, 117.79, 112.51, 111.68; LC/MS (M + H$^+$) 394; HRMS (ESI-Orbitrap) calcd for $C_{22}H_{28}N_5O_2$ [M + H$^+$]: 394.2243, found 394.2240.

1-(4-(1H-Pyrazol-4-yl)phenyl)-3-(3-methoxybenzyl)-1-(2-(pyrrolidin-1-yl)ethyl)urea (**8d**). 39% yield in four steps. ^{1}H NMR (DMSO-d_6, 400 MHz) δ 9.46 (br, s, 1H), 8.11 (s, 2H), 7.72 (d, J = 8.4 Hz, 2H), 7.35 (d, J = 8.4 Hz, 2H), 7.22−7.18 (m, 1H), 6.80−6.76 (m, 3H), 6.44 (t, J = 6.0 Hz, 1H), 4.17 (d, J = 6.0 Hz, 2H), 3.92 (dd, J = 12.4, 6.4 Hz, 2H), 3.72 (s, 3H), 3.68−3.61 (m, 2H), 3.24 (dd, J = 12.4, 6.4 Hz, 2H), 3.08−3.01 (m, 2H), 2.02−1.97 (m, 2H), 1.87−1.84 (m, 2H); ^{13}C NMR (DMSO-d_6, 100 MHz) δ 159.13, 158.30, 157.97, 157.01, 142.42, 138.57, 132.32, 129.08, 128.82, 126.49, 120.46, 119.04, 112.53, 111.67, 54.87, 53.63, 52.47, 45.51, 43.60, 22.52; LC/MS (M + H$^+$) 420; HRMS (ESI-Orbitrap) calcd for $C_{24}H_{30}N_5O_2$ [M + H$^+$]: 420.2400, found 420.2396.

1-(4-(1H-Pyrazol-4-yl)phenyl)-1-(3-(dimethylamino)propyl)-3-(3-methoxybenzyl)urea (**8e**). 64% yield in three steps. ^{1}H NMR (DMSO-d_6, 400 MHz) δ 9.40 (s, br, 1H), 8.10 (s, 2H), 7.69 (d, J = 8.4 Hz, 2H), 7.30 (d, J = 8.4 Hz, 2H), 7.22−7.19 (m, 1H), 6.80−6.75 (m, 3H), 6.35 (t, J = 6.0 Hz, 1H), 4.15 (d, J = 6.0 Hz, 2H), 3.73 (s, 3H), 3.67−3.63 (m, 2H), 3.08−3.02 (m, 2H), 2.74 (s, 6H), 1.80−1.73 (m, 2H); ^{13}C NMR (DMSO-d_6, 100 MHz) δ 159.14, 158.44, 158.09, 157.06, 142.59, 138.82, 132.04, 129.08, 128.88, 126.39, 120.52, 118.97, 112.46, 111.63, 54.87, 54.29, 45.80, 43.56, 42.11, 23.18; LC/MS (M + H$^+$): 408; HRMS (ESI-Orbitrap) calcd for $C_{23}H_{30}N_5O_2$ [M + H$^+$]: 408.2400, found 408.2409.

3-(4-(1H-Pyrazol-4-yl)phenyl)-1-(3-methoxybenzyl)-1-methylurea (**12a**). 69% yield in three steps. ^{1}H NMR (DMSO-d_6, 400 MHz) δ 8.38 (s, 1H), 7.96 (s, 2H), 7.48−7.47 (m, 4H), 7.29−7.25 (m, 1H), 6.84−6.82 (m, 3H), 4.52 (s, 2H), 3.74 (s, 3H), 2.92 (s, 3H); ^{13}C NMR (DMSO-d_6, 100 MHz) δ 159.40, 155.63, 140.11, 138.49, 129.55, 126.58, 124.99, 121.10, 120.20, 119.36, 113.01, 112.15, 54.93, 51.18, 34.36; LC/MS (M + H$^+$) 337; HRMS (ESI-Orbitrap) calcd for $C_{19}H_{21}N_4O_2$ [M + H$^+$]: 337.1665, found 337.1653.

3-(4-(1H-Pyrazol-4-yl)phenyl)-1-ethyl-1-(3-methoxybenzyl)urea (**12b**). 72% yield in three steps. ^{1}H NMR (DMSO-d_6, 400 MHz) δ 12.82 (br, s, 1H), 8.33 (s, 1H), 8.08 (s, 1H), 7.84 (s, 1H), 7.47−7.46 (m, 4H), 7.28−7.24 (m, 1H), 6.86−6.81 (m, 3H), 4.54 (s, 2H), 3.73 (s, 3H), 3.35 (q, J = 3.2 Hz, 2H), 1.07 (t, J = 3.2 Hz, 3H); ^{13}C NMR (DMSO-d_6, 100 MHz) δ 159.35, 155.01, 140.66, 138.49, 135.80, 129.46, 126.57, 124.96, 124.56, 121.11, 120.34, 119.33, 113.00, 112.05, 54.93, 48.66, 40.80, 13.36; LC/MS (M + H$^+$) 351.06; HRMS (ESI-Orbitrap) calcd for $C_{20}H_{23}N_4O_2$ [M + H$^+$]: 351.1821, found 351.1809.

3-(4-(1H-Pyrazol-4-yl)phenyl)-1-cyclopropyl-1-(3-methoxybenzyl)urea (**12c**). 75% yield in three steps. ^{1}H NMR (DMSO-d_6, 400 MHz) δ 8.30 (s, 1H), 7.98 (s, 2H), 7.54−7.48 (m, 4H), 7.27−7.23 (m, 1H), 6.84−6.81 (m, 3H), 4.50 (s, 2H), 3.73 (s, 3H), 2.62−2.58 (m, 1H), 0.89−0.86 (m, 2H), 0.76−0.73 (m, 2H); ^{13}C NMR (DMSO-d_6, 100 MHz) δ 159.32, 158.45, 156.04, 140.82, 138.01, 130.26, 129.46, 126.78, 125.08, 121.11, 120.06, 119.28, 112.96, 111.88, 54.90, 49.59, 28.20, 8.95; LC/MS (M + H$^+$) 363; HRMS (ESI-Orbitrap) calcd for $C_{21}H_{23}N_4O_2$ [M + H$^+$]: 363.1821, found 363.1808.

3-(4-(1H-Pyrazol-4-yl)phenyl)-1-isopropyl-1-(3-methoxybenzyl)-urea (**12d**). 70% yield in three steps. ^{1}H NMR (DMSO-d_6, 400 MHz) δ 8.22 (s, 1H), 7.95 (s, 2H), 7.46−7.40 (m, 4H), 7.25−7.21 (m, 1H), 6.87−6.84 (m, 2H), 6.79−6.76 (m, 1H), 4.51 (s, 2H), 4.50−4.49 (m, 1H), 3.72 (s, 3H), 1.09 (s, 6H); ^{13}C NMR (DMSO-d_6, 100 MHz) δ 159.20, 158.00, 155.22, 142.28, 138.49, 130.30; 129.22, 126.51, 124.94, 121.09, 120.28, 118.64, 112.32, 111.49, 54.88, 46.42, 43.92, 20.75; LC/MS (M + H$^+$) 365; HRMS (ESI-Orbitrap) calcd for $C_{21}H_{25}N_4O_2$ [M + H$^+$]: 365.1978, found 365.1965.

3-(4-(1H-Pyrazol-4-yl)phenyl)-1-(2-hydroxyethyl)-1-(3-methoxybenzyl)urea (**12e**). 68% yield in three steps. ^{1}H NMR (DMSO-d_6, 400 MHz)δ 12.82 (br, s, 1H), 8.67 (s, 1H), 7.95 (br, s, 2H), 7.47 (dd, J = 6.8, 2.0 Hz, 2H), 7.40 (dd, J = 6.8, 2.0 Hz, 2H), 7.28−7.24 (m, 1H), 6.87−6.81 (m, 3H), 5.26 (br, s, 1H), 4.57 (s, 2H), 3.74 (s, 3H), 3.57 (t, J = 5.6 Hz, 2H), 3.38 (t, J = 5.6 Hz, 2H); ^{13}C NMR (DMSO-d_6, 100 MHz) δ 159.35, 157.63, 155.81, 157.20, 140.57, 138.44, 129.46, 126.47, 125.13, 121.08, 119.67, 119.41, 113.07, 112.06, 59.90, 54.92, 49.91, 49.00; LC/MS (M + H$^+$) 367; HRMS (ESI-Orbitrap) calcd for $C_{20}H_{23}N_4O_3$ [M + H$^+$]: 367.1770, found 367.1758.

3-(4-(1H-Pyrazol-4-yl)phenyl)-1-(3-methoxybenzyl)-1-(2-methoxyethyl)urea (**12f**). 72% yield in three steps. ^{1}H NMR (DMSO-d_6, 400 MHz) δ 8.41 (s, 1H), 7.96 (s, 2H), 7.47 (d, J = 8.8 Hz, 2H), 7.41 (d, J = 8.8 Hz, 2H), 7.28−7.24 (m, 1H), 6.85−6.82 (m, 3H), 4.58 (s, 2H), 3.73 (s, 3H), 3.47 (s, 3H), 3.28−3.27 (m, 4H); ^{13}C NMR (DMSO-d_6, 100 MHz) δ 159.37, 158.50, 155.45, 140.42, 138.32, 130.68, 129.49, 126.58, 125.08, 121.08, 119.95, 119.25, 112.92, 112.11, 70.80, 58.28, 54.93, 49.88, 46.06; LC/MS (ESI, M + H$^+$) 381; HRMS calcd for $C_{21}H_{25}N_4O_3$ [M + H$^+$]: 381.1927, found 381.1913.

3-(4-(1H-Pyrazol-4-yl)phenyl)-1-(2-aminoethyl)-1-(3-methoxybenzyl)urea (**12g**). The synthesis started from *N*-Boc-protected ethyl diamine. After Suzuki reaction, the organic solvent of the reaction mixture was removed under reduced pressure and remaining residue was treated with TFA (0.4 mL) in DCM (0.6 mL). One half hour later the mixture was submitted for the preparative HPLC to give **12g** as a white solid in 57% overall yield (four steps). ^{1}H NMR (DMSO-d_6, 400 MHz) δ 8.54 (s, 1H), 7.97 (s, 1H), 7.74 (br, s, 3H), 7.51−7.46 (m, 4H), 7.33−7.29 (m, 1H), 6.88−6.83 (m, 3H), 4.65 (s, 2H), 3.75 (s, 3H), 3.48 (t, J = 6.0 Hz, 2H), 2.98 (t, J = 6.0 Hz, 2H); ^{13}C NMR (DMSO-d_6, 100 MHz) δ 159.46, 158.47, 158.13,

dx.doi.org/10.1021/jm400062r | J. Med. Chem. XXXX, XXX, XXX−XXX

155.59, 139.64, 138.02, 129.73, 126.99, 124.97, 121.01, 120.64, 119.08, 112.94, 112.28, 54.98, 49.73, 43.90, 37.46; LC/MS (M + H^+) 366; HRMS (ESI-Orbitrap) calcd for $C_{20}H_{24}N_5O_2$ [M + H^+]: 366.1930, found 366.1918.

3-(4-(1H-Pyrazol-4-yl)phenyl)-1-(2-(dimethylamino)ethyl)-1-(3-methoxybenzyl)urea (**12h**). 75% yield in three steps. ^{1}H NMR (DMSO-d_6, 400 MHz) δ 9.17 (br, s, 1H), 8.61 (s, 1H), 7.98 (s, 2H), 7.50−7.47 (m, 4H), 7.34−7.30 (m, 1H), 6.89−6.83 (m, 3H), 4.67 (s, 2H), 3.75 (s, 3H), 3.59 (t, J = 6.4 Hz, 2H), 3.26 (t, J = 6.4 Hz, 2H), 2.84 (s, 3H), 2.83 (s, 3H); ^{13}C NMR (DMSO-d_6, 100 MHz) δ 159.50, 158.21, 157.90, 155.64, 139.34, 137.86, 129.77, 127.14, 124.98, 120.96, 120.70, 119.03, 112.86, 112.35, 54.99, 54.55, 49.26, 42.71, 41.24; LC/MS (M + 1) 394; HRMS (ESI-Orbitrap) calcd for $C_{22}H_{28}N_5O_2$ [M + H^+]: 394.2243, found 394.2229.

3-(4-(1H-Pyrazol-4-yl)phenyl)-1-(3-methoxybenzyl)-1-(2-(pyrrolidin-1-yl)ethyl)urea (**12i**). 78% yield in three steps. ^{1}H NMR (DMSO-d_6, 400 MHz) δ 9.41 (br, s, 1H), 8.61 (s, 1H), 7.96 (s, 1H), 7.50−7.45 (m, 4H), 7.34−7.30 (m, 1H), 6.89−6.83 (m, 3H), 4.68 (s, 2H), 3.75 (s, 3H), 3.61−3.57 (m, 4H), 3.39−3.31 (m, 2H), 3.09−3.01 (m, 2H), 2.02−2.00 (m, 2H), 1.90−1.84 (m, 2H); ^{13}C NMR (DMSO-d_6, 100 MHz) δ 159.46, 158.60, 158.25, 155.36, 139.56, 138.04, 129.70, 126.91, 124.97, 121.06, 120.62, 119.14, 112.94, 112.34, 54.97, 53.31, 51.58, 49.49, 42.36, 22.64; LC/MS (M + 1) 420; HRMS (ESI-Orbitrap) calcd for $C_{24}H_{30}N_5O_2$ [M + H^+]: 420.2400, found 420.2394.

3-(4-(1H-Pyrazol-4-yl)phenyl)-1-(3-methoxybenzyl)-1-(3-(pyrrolidin-1-yl)propyl)urea (**12j**). 75% yield in three steps. ^{1}H NMR (DMSO-d_6, 400 MHz) δ 9.53 (s. br, 1H), 8.47 (s, 1H), 7.96 (s, 2H), 7.50−7.44 (m, 4H), 7.32−7.28 (m, 1H), 6.87−6.83 (m, 3H), 4.61 (s, 2H), 3.74 (s, 3H), 3.54−3.50 (m, 2H), 3.37−3.34 (m, 2H), 3.14−3.09 (m, 2H), 3.01−2.93 (m, 2H), 2.01−1.99 (m, 2H), 1.90−1.84 (m, 4H); ^{13}C NMR (DMSO-d_6, 100 MHz) δ 159.44, 158.53, 158.18, 155.36, 140.06, 138.16, 129.64, 126.86, 124.98, 121.04, 120.60, 119.14, 112.17, 111.88, 54.95, 53.18, 51.72, 49.31, 43.38, 24.36, 22.56; LC/MS (M + 1) 434; HRMS (ESI-Orbitrap) calcd for $C_{25}H_{32}N_5O_2$ [M + H^+]: 434.2556, found 434.2559.

3-(4-(1H-Pyrazol-4-yl)phenyl)-1-(3-methoxybenzyl)-1-(2-morpholinoethyl)urea (**12k**). 73% yield in three steps. ^{1}H NMR (DMSO-d_6, 400 MHz) δ 9.59 (br, s, 1H), 8.64 (s, 1H), 7.97 (s, 2H), 7.51−7.45 (m, 4H), 7.34−7.30 (m, 1H), 6.89−6.83 (m, 3H), 4.68 (s, 2H), 4.02−3.97 (m, 2H), 3.75 (s, 3H), 3.66−3.60 (m, 4H), 3.57−3.52 (m, 2H), 3.33−3.30 (m, 2H), 3.13−3.11 (m, 2H); ^{13}C NMR (DMSO-d_6, 100 MHz) δ 159.51, 158.35, 158.02, 155.63, 139.29, 137.83, 129.78, 127.14, 124.99, 120.97, 120.71, 119.02, 112.85, 112.35, 63.33, 55.00, 53.77, 51.50, 49.38, 40.58; LC/MS (M + H^+) 436; HRMS (ESI-Orbitrap) calcd for $C_{24}H_{30}N_5O_3$ [M + H^+]: 436.2349, found 436.2333.

3-(4-(1H-Pyrazol-4-yl)phenyl)-1-(3-methoxybenzyl)-1-(3-morpholinopropyl)urea (**12l**). 64% yield in three steps. ^{1}H NMR (DMSO-d_6, 400 MHz) δ 9.62 (s, br, 1H), 8.49 (s, 1H), 7.96 (s, 2H), 7.50−7.44 (m, 4H), 7.32−7.28 (m, 1H), 6.88−6.83 (m, 3H), 4.62 (s, 2H), 3.99−3.96 (m, 2H), 3.74 (s, 3H), 3.66−3.60 (m, 2H), 3.43−3.40 (m, 2H), 3.37−3.33 (m, 2H), 3.10−3.04 (m, 4H), 1.95−1.90 (m, 2H); ^{13}C NMR (DMSO-d_6, 100 MHz) δ 159.45, 158.32, 157.99, 155.38, 139.93, 138.11, 129.68, 126.91, 124.97, 121.01, 120.59, 119.10, 112.91, 112.17, 66.31, 63.36, 54.98, 53.74, 51.11, 49.27, 22.12; LC/MS (M + H^+) 450; HRMS (ESI-Orbitrap) calcd for $C_{25}H_{32}N_5O_3$ [M + H^+]: 450.2505, found 450.2509.

3-(4-(1H-Pyrazol-4-yl)phenyl)-1-(3-methoxybenzyl)-1-(2-(piperidin-1-yl)ethyl)urea (**12m**). 70% yield in three steps. ^{1}H NMR (DMSO-d_6, 400 MHz) δ 9.00 (s, br, 1H), 8.63 (s, 1H), 7.97 (s, 2H), 7.51−7.45 (m, 4H), 7.34−7.30 (m, 1H), 6.89−6.83 (m, 3H), 4.67 (s, 2H), 3.75 (s, 3H), 3.62−3.59 (m, 2H), 3.53−3.50 (m, 2H), 3.25−3.21 (m, 2H), 2.95−2.87 (m, 2H), 1.83−1.80 (m, 2H), 1.70−1.56 (m, 3H), 1.41−1.35 (m, 1H); ^{13}C NMR (DMSO-d_6, 100 MHz) δ 159.51, 158.22, 157.89, 155.63, 139.36, 137.84, 129.79, 127.14, 125.00, 120.96, 120.68, 119.04, 112.87, 112.35, 55.01, 53.60, 52.51, 49.50, 41.00, 22.54, 21.14; LC/MS (M + H^+): 434; HRMS (ESI-Orbitrap) calcd for $C_{25}H_{32}N_5O_2$ [M + H^+]: 434.2556, found 434.2565.

3-(4-(1H-Pyrazol-4-yl)phenyl)-1-(3-methoxybenzyl)-1-(3-(piperidin-1-yl)propyl)urea (**12n**). 72% yield in three steps. ^{1}H NMR (DMSO-d_6, 400 MHz) δ 9.08 (s, br, 1H), 8.49 (s, 1H), 7.97 (s, 2H), 7.50−7.45 (m, 4H), 7.33−7.29 (m, 1H), 6.88−6.84 (m, 3H), 4.62 (s, 2H), 3.75 (s, 3H), 3.42−3.40 (m, 2H), 3.36−3.33 (m, 2H), 3.05−3.00 (m, 2H), 2.90−2.81 (m, 2H), 1.95−1.87 (m, 2H), 1.83−1.79 (m, 2H), 1.71−1.57 (m, 3H), 1.42−1.34 (m, 1H); ^{13}C NMR (DMSO-d_6, 100 MHz) δ 159.44, 158.38, 158.05, 155.39, 139.99, 138.14, 129.66, 126.89, 124.97, 121.04, 120.59, 119.15, 112.94, 112.17, 54.97, 53.51, 52.05, 49.21, 43.40, 22.54, 22.35, 21.21; LC/MS (M + H^+): 448; HRMS (ESI-Orbitrap) calcd for $C_{26}H_{34}N_5O_2$ [M + H^+]: 448.2713, found 448.2718.

3-(4-(1H-Pyrazol-4-yl)phenyl)-1-benzyl-1-(2-hydroxyethyl)urea (**12o**). 62% in three steps. ^{1}H NMR (400 MHz, DMSO-d_6) δ 8.69 (s, 1H), 7.96 (s, 2H), 7.48 (d, J = 8.7 Hz, 2H), 7.40 (d, J = 8.7 Hz, 2H), 7.37 − 7.31 (m, 2H), 7.27 (dd, J = 14.6, 7.1 Hz, 3H), 4.60 (s, 2H), 3.56 (t, J = 5.4 Hz, 3H), 3.37 (t, J = 5.3 Hz, 2H), 2.07 (s, 1H). LC/MS calcd for $C_{19}H_{20}N_4O_2$ (M + H^+): 337, found 337.

1-Benzyl-3-(2-fluoro-4-(1H-pyrazol-4-yl)phenyl)-1-(2-hydroxyethyl)urea (**12p**). 56% in three steps. ^{1}H NMR (400 MHz, DMSO-d_6) δ 12.91 (s, 1H), 8.86 (s, 1H), 8.17 (s, 1H), 7.92 (s, 1H), 7.72 (t, J = 8.5 Hz, 1H), 7.47 (dd, J = 12.5, 1.9 Hz, 1H), 7.39 − 7.19 (m, 5H), 5.62 (s, 1H), 4.56 (s, 2H), 3.58 (dd, J = 9.0, 4.3 Hz, 2H), 3.41 − 3.26 (m, 6H), 2.08 (d, J = 4.2 Hz, 1H). LC/MS calcd for $C_{19}H_{19}FN_4O_2$ (M + H^+): 355, found 355.

1-(4-(1H-Pyrazol-4-yl)phenyl)-3-(3-hydroxy-1-(3-methoxyphenyl)propyl)urea (**14a**). 79% yield in two steps. ^{1}H NMR (DMSO-d_6, 400 MHz) δ 8.45 (s, 1H), 7.98 (s, 2H), 7.44 (d, J = 8.8 Hz, 2H), 7.34 (d, J = 8.8 Hz, 2H), 7.27−7.23 (m, 1H), 6.90−6.87 (m, 2H), 6.81−6.79 (m, 1H), 6.69−6.66 (m, 1H), 4.84−4.79 (m, 2H), 3,75 (s, 3H), 3.46−3.38 (m, 2H), 1.86−1.81 (m, 2H); ^{13}C NMR (DMSO-d_6, 100 MHz) δ 159.23, 154.58, 146.07, 138.42, 129.27, 125.83, 125.52, 125.41, 121.14, 118.56, 118.42, 117.90, 112.13, 111.63, 57.75, 54.92, 50.44, 32.46; LC/MS (M + H^+): 367; HRMS (ESI-Orbitrap) calcd for $C_{23}H_{30}N_5O_2$ [M + H^+]: 367.1770, found 367.1762.

1-(4-(1H-Pyrazol-4-yl)phenyl)-3-(1-(3-fluorophenyl)-3-hydroxypropyl)urea (**14b**). 76% yield in two steps. ^{1}H NMR (DMSO-d_6, 400 MHz) δ 8.48 (s, 1H), 7.93 (s, 2H), 7.43 (d, J = 8.8 Hz, 2H), 7.40−7.36 (m, 1H), 7.34 (d, J = 8.8 Hz, 2H), 7.16−7.11 (m, 2H), 7.07−7.02 (m, 1H), 6.72 (d, J = 7.6 Hz, 1H), 4.89−4.83 (m, 1H), 3.46−3.37 (m, 2H), 1.86−1.81 (m, 2H); LC/MS (M + H^+) 355; HRMS (ESI-Orbitrap) calcd for $C_{19}H_{20}FN_4O_2$ [M + H^+]: 355.1570, found 355.1587.

1-(4-(1H-Pyrazol-4-yl)phenyl)-3-(3-hydroxy-1-phenylpropyl)urea (**14c**). 81% yield in two steps. ^{1}H NMR (DMSO-d_6, 400 MHz) δ 8.44 (s, 1H), 7.93 (s, 2H), 7.44−7.42 (m, 2H), 7.35−7.30 (m, 7H), 7.24−7.20 (m, 1H), 6.67 (d, J = 8.0 Hz, 1H), 4.86−4.81 (m, 1H), 3.46−3.35 (m, 2H), 1.86−1.81 (m, 2H); ^{13}C NMR (DMSO-d_6, 100 MHz) δ 161.25, 158.42, 158.06, 154.55, 144.36, 138.41, 130.10, 128.20, 126.51, 126.18, 125.79, 125.40, 121.12, 117.86, 57.73, 50.44, 31.58; LC/MS (M + H^+) 337; HRMS (ESI-Orbitrap) calcd for $C_{19}H_{21}N_4O_2$ [M + H^+]: 337.1665, found 337.1660.

1-(4-(1H-Pyrazol-4-yl)phenyl)-3-(2-hydroxy-1-phenylethyl)urea (**14d**). 75% yield in two steps. ^{1}H NMR (DMSO-d_6, 400 MHz) δ 12.81 (s, br, 1H), 8.62 (s, 1H), 7.83−7.78 (m, 2H), 7.45−7.43 (m, 2H), 7.35−7.32 (m, 6H), 7.25−7.22 (m, 1H), 6.67 (d, J = 7.6 Hz, 1H), 4.97 (s, br, 1H), 4.77−4.72 (m, 1H), 3.70−3.59 (m, 2H); ^{13}C NMR (DMSO-d_6, 100 MHz) δ 154.71, 142.12, 138.40, 130.10, 128.03, 126.68, 126.61, 125.87, 125.43, 121.09, 117.79, 113.79, 64.94, 55.00; LC/MS (M + H^+) 323; HRMS (ESI-Orbitrap) calcd for $C_{18}H_{19}N_4O_2$ [M + H^+]: 323.1508, found 323.1500.

1-(4-(1H-Pyrazol-4-yl)phenyl)-3-(3-(dimethylamino)-1-phenylpropyl)urea (**14e**). 69% yield in two steps. ^{1}H NMR (DMSO-d_6, 400 MHz) δ 9.45 (s, br, 1H), 8.59 (s, 1H), 7.94 (s, 2H), 7.46−7.42 (m, 2H), 7.40−7.35 (m, 6H), 7.32−7.28 (m, 1H), 4.85−4.79 (m, 1H), 3.17−3.01 (m, 2H), 2.79 (s, 6H), 2.14−2.07 (m, 2H); ^{13}C NMR (DMSO-d_6, 100 MHz) δ 158.71, 158.36, 154.71, 142.78, 138.29, 128.54, 127.22, 126.29, 125.97, 125.41, 121.08, 117.94, 54.67, 50.84, 42.49, 31.13; LC/MS (M + H^+) 364; HRMS (ESI-Orbitrap) calcd for $C_{21}H_{26}N_5O$ [M + H^+]: 364.2137, found 364.2129.

(S)-1-Ethyl-1-(3-methoxybenzyl)-3-(2-(1-methylpyrrolidin-3-yloxy)-4-(1H-pyrazol-4-yl)-phenyl)urea (**19a**). 65% yield in four steps. ^{1}H NMR (DMSO-d_6, 400 MHz) δ 10.04 (s, br, 1H), 8.05 (s, 2H), 7.68−7.54 (m, 2H), 7.32−7.28 (m, 1H), 7.19−7.15 (m, 2H),

dx.doi.org/10.1021/jm400062r | J. Med. Chem. XXXX, XXX, XXX−XXX

6.90−6.86 (m, 3H), 5.32−5.22 (m, 1H), 4.58−4.55 (m, 2H), 4.05−3.98 (m, 1H), 3.76 (s, 3H), 3.43−3.37 (m, 2H), 3.18−3.11 (m, 2H), 2.89−2.85 (m, 3H), 2.59−2.54 (m, 1H), 2.26−2.14 (m, 1H), 2.08−2.01 (m, 1H, 1.15−1.10 (m, 3H); ^{13}C NMR (DMSO-d_6, 100 MHz) δ 159.43, 158.50, 158.17, 154.98, 148.09, 147.01, 140.37, 129.64, 126.86, 122.62, 120.97, 119.02, 117.75, 112.90, 112.04, 109.48, 75.19, 59.70, 54.98, 53.91, 53.16, 49.04, 41.55, 31.08, 13.25; LC/MS (M + H$^+$) 450; HRMS (ESI-Orbitrap) calcd for $C_{25}H_{32}N_5O_3$ [M + H$^+$]:450.2505, found 450.2513.

*3-(2-(2-Hydroxyethoxy)-4-(1H-pyrazol-4-yl)phenyl)-1-(2-hydroxyethyl)-1-(3-methoxybenzyl)-urea (**19b**).* ^{1}H NMR (400 MHz, DMSO-d_6) δ 8.46 (d, J = 24.5 Hz, 1H), 8.02 (s, 2H), 7.85 (t, J = 6.0 Hz, 1H), 7.26 (t, J = 7.9 Hz, 1H), 7.21 (d, J = 1.8 Hz, 1H), 7.12 (dd, J = 8.3, 1.8 Hz, 1H), 6.90 (d, J = 7.3 Hz, 2H), 6.83 (dd, J = 7.3, 1.8 Hz, 1H), 4.53 (s, 2H), 4.07 (t, J = 5.1 Hz, 2H), 3.77 − 3.70 (m, 5H), 3.60 (t, J = 4.9 Hz, 2H), 3.37 (t, J = 4.7 Hz, 2H). LC/MS calcd for $C_{22}H_{26}N_4O_5$ (M + H$^+$): 427, found 427.

*3-(2-(2-(Dimethylamino)ethoxy)-4-(1H-pyrazol-4-yl)phenyl)-1-(2-(dimethylamino)ethyl)-1-(3-methoxybenzyl)urea (**19c**).* 57% yield in four steps. ^{1}H NMR (DMSO-d_6, 400 MHz) δ 9.77−9.45 (m, 1H), 8.05 (s, 2H), 7.80 (s, 1H), 7.59−7.57 (m, 1H), 7.40−7.36 (m, 1H), 7.29−7.28 (m, 1H), 7.22−7.19 (m, 1H), 6.94−6.87 (m, 3H), 4.69 (s, 2H), 4.41−4.38 (m, 2H), 3.78 (s, 3H), 3.65−3.62 (m, 2H), 3.36−3.35 (m, 2H), 3.29−3.28 (m, 2H), 2.85 (s, 6H), 2.77 (s, 6H); ^{13}C NMR (DMSO-d_6, 100 MHz) δ 160.52, 159.43, 159.10, 156.68, 150.14, 139.96, 130.95, 130.39, 126.72, 124.92, 121.87, 119.75, 118.64, 113.80, 113.28, 110.17, 63.28, 56.40, 56.03, 55.42, 50.49, 43.65, 43.49, 42.69; LC/MS (M + H$^+$): 481; HRMS (ESI-Orbitrap) calcd for $C_{26}H_{37}N_6O_3$ [M + H$^+$]: 481.2927, found 481.2935.

*3-(5-(1H-Pyrazol-4-yl)pyridin-2-yl)-1-(2-(dimethylamino)ethyl)-1-(3-methoxybenzyl)urea (**20**).* 70% yield in three steps. ^{1}H NMR (DMSO-d_6, 400 MHz) δ 9.17 (br, s, 1H), 8.61 (s, 1H), 7.98 (s, 2H), 7.50−7.47 (m, 4H), 6.89−6.83 (m, 3H), 4.67 (s, 2H), 3.75 (s, 3H), 3.59 (t, J = 6.4 Hz, 2H), 3.26 (t, J = 6.4 Hz, 2H), 2.84 (s, 3H), 2.83 (s, 3H); LC/MS (M + 1) 395; HRMS (ESI-Orbitrap) calcd for $C_{21}H_{27}N_6O_2$ [M + H$^+$]: 395.2195, found 395.2176.

ROCK-I/II Assays.[34] Assays were performed using the STK2 kinase system from Cisbio. A 5 μL mixture of a 1 μM STK2 substrate and ATP (ROCK-I: 4 μM, ROCK-II: 20 μM) in STK-buffer was added to the wells of the 384-well plate using a BioRAPTR FRD Workstation (Aurora Discovery, Carlsbad, CA). Twenty nanoliters of test compound was then dispensed using a 384-head offline Pintool system (GNF Systems, San Diego, CA). The reaction was started by adding either 5 μL of 2.5 nM ROCK-I (Upstate #14-601) or 5 μL of 0.5 nM ROCK-II in STK-buffer. After 4h at RT the reaction was stopped by adding 10 μL of 1X antibody and 62.5 nM Sa-XL in Detection Buffer. After 1 h incubation at RT, the plates were read on the Viewlux in HTRF mode.

PKA Assay.[35] A 5 μL mixture of 60 μM kemptide and 20 μM ATP in kinase buffer (50 mM HEPES pH 7.3, 10 mM $MgCl_2$, 0.1% BSA, 2 mM DTT) was added to the wells using a BioRAPTR FRDTM Workstation (Aurora Discovery, Carlsbad, CA). Twenty nanoliters of test compound was then dispensed using a 384-head offline Pintool system (GNF Systems, San Diego, CA). The reaction was started by adding 5 μL of 0.5 nM PKA (Upstate #14-440) in kinase buffer (5 μL of kinase buffer was used for high wells). After 70 min incubation at RT, the reaction was stopped by adding 10 μL Kinase-Glo reagent and the plate was read after 10 min incubation at RT on the Viewlux in luminescence mode.

ppMLC Assay. A7r5 cells obtained from ATCC (Manassas, VA) were maintained in 20% FBS supplemented DMEM at 5% CO_2, 37 °C, in a humid environment and plated in clear-bottomed Packard View plates ((Perkin-Elmer, Waltham, MA) at 5000 cells/well and allowed to attach overnight. Serum starvation was performed by media change to DMEM/0.05% FBS for 4 h. The cells were then treated with 13333 nM to 18 nM final compound concentration along with DMSO control for 1 h, followed by treatment with 10 μM L-α-lysophosphatidic acid (LPA, Sigma-Aldrich) for 10 min. Cells were fixed in 4% paraformaldehyde for 25 min, washed with 0.1 M glycine, permeabilized with 0.2% Triton-X for 20 min, washed with PBS, blocked with Licor Blocking Buffer (LI-COR Biosciences, diluted 1:1 in PBS) for 1.5 h, and incubated with anti-PP-MLC (Cell Signaling) at 1:200 dilution overnight at 4 °C with rocking. Plates were then washed twice with PBS/0.05% Tween 20 and once with Licor Blocking Buffer/PBS/0.05% Tween 20. Secondary antibody incubation was performed with Goat-anti-Rabbit IR 800 (LI-COR Biosciences) used at 1:500 dilution in Licor Blocking Buffer/PBS/0.05% Tween 20 for 1 h at RT with rocking, followed by washing twice with PBS/0.05% Tween 20 and once with Licor Blocking Buffer/PBS/0.05%. Nuclear staining was performed with TO-PRO-3 iodide (642/661) (Invitrogen) diluted at 1:4000 in LI-COR Buffer/PBS for 30 min at RT with rocking, followed by washing twice with PBS. The ppMLC and nuclear signal was determined by reading the plate on an Odyssey LI-COR Infrared Scanner (LI-COR Biosciences at 800 and 700 nm channels, respectively, and collecting the RAW data. The final percentage of ppMLC phosphorylation was derived by normalizing the signal in each well to its corresponding nuclear fluorescence.

Molecular Modeling. The homology model of human Rock2 was constructed using Prime v3.1 (Schrodinger, LLC, New York, NY) with the option of a single template to build a single chain. The crystal structure of Bovine Rock2 (PDB ID 2F2U), which shows sequence identity over 92%, was used as a template for the model, and the final model also included the ligand of the template, Fasudil. The model was further prepared through protein preparation wizard in Maestro v9.3 (Schrodinger, LLC). Docking studies were performed using Glide SP v5.8 (Schrodinger, LLC) with one hydrogen bond constraint to either the carbonyl oxygen of Glu 170 or amino group of Met 172 in the hinge region. The docking grid was generated around the model ligand Fasudil with a box size of 20 × 20 × 20 Å^3. Each inhibitor compound was prepared for Glide docking with LigPrep v2.5 (Schrodinger, LLC) to include different conformational states. The docking pose with the highest docking score for each inhibitor compound was then merged to the human Rock2 model for energy minimization using the OPLS2005 force field (Schrodinger, LLC).

■ ASSOCIATED CONTENT

Ⓢ Supporting Information

Details for the synthetic procedure of **6b−f**; LC purity data, protocols for JNKs, MRCKα, and p38α enzyme assays; procedures for DMPK studies. This material is available free of charge via the Internet at http://pubs.acs.org/

■ AUTHOR INFORMATION

Corresponding Author

*(Y.F.) E-mail: yfeng@scripps.edu; phone: 561-228-2201; fax: 561-228-3089. (P.L.) E-mail: lograsso@scripps.edu; phone: 561-228-2230; fax: 561-228-3089.

Present Address

[#]School of Chemical and Environmental Engineering, Shanghai Institute of Technology, 100 Hai Quan Rd., Shanghai, P.R. China 201418.

Notes

The authors declare no competing financial interest.

■ ACKNOWLEDGMENTS

We are grateful to Dr. Derek Duckett and Ms. Weimin Chen for p38α and JNK assays, Dr. Michael Chalmers for HRMS, and Dr. Ke Zheng for the ^{1}H NMR characterization of **12o**, **12p**, and **19b**. This research was also partially supported by the Shanghai Municipal Natural Science Foundation (12ZR1431100, to Y.Y).

■ ABBREVIATIONS USED

AUC, pharmacokinetic area under curve; Cl, pharmacokinetic clearance; C_{max}, pharmacokinetic maximum concentration; F%,

oral bioavailability; HLMS, human liver microsomal stability; ppMLC, bis-phospho myosin light chain; V_d, volume of distribution; IOP, intraocular pressure; ROCK, Rho-associated coiled-coil protein kinase; SAR, structure−activity relationship; DMPK, drug metabolism and pharmacokinetics; DCM, dichloromethane; HATU, 2-(1*H*-7-azabenzotriazol-1-yl)-1,1,3,3-tetramethyluronium hexafluorophosphate methanaminium; DMF, *N*,*N*-dimethylformamide; HPLC, high pressure liquid chromatography; DCM, dichloromethane

REFERENCES

(1) Nakagawa, O.; Fujisawa, K.; Ishizaki, T.; Saito, Y.; Nakao, K.; Narumiya, S. ROCK-I and ROCK-II, two isoforms of Rho-associated coil-coil forming protein serine/threonine kinase in mice. *FEBS Lett.* **1996**, *392*, 189−193.

(2) Uehata, M.; Ishizaki, T.; Satoh, H.; Ono, T.; Kawahara, T.; Morishita, T.; Tamakawa, H.; Yamagami, K.; Inui, J.; Maekawa, M.; Narumiya, S. Calcium sensitization of smooth muscle mediated by a Rho-associated protein kinase in hypertension. *Nature* **1997**, *389*, 990−994.

(3) Rikitake, Y.; Kim, H. H.; Huang, Z. H.; Seto, M.; Yano, K.; Asano, T.; Moskowitz, M. A.; Liao, J. K. Inhibition of Rho kinase (ROCK) leads to increased cerebral blood flow and stroke protection. *Stroke* **2005**, *36*, 2251−2257.

(4) Sun, H.; Breslin, J. W.; Zhu, J.; Yuan, S. Y.; Wu, M. H. Rho and ROCK signaling in VEGF-induced microvascular endothelial hyperpermeability. *Microcirculation* **2006**, *13*, 237−247.

(5) Nakajima, E.; Nakajima, T.; Minagawa, Y.; Shearer, T. R.; Azuma, M. Contribution of ROCK in contraction of trabecular meshwork: proposed mechanism for regulating aqueous outflow in monkey and human eyes. *J. Pharm. Sci.* **2005**, *47*, 701−708.

(6) Ying, H.; Biroc, S. L.; Li, W.; Alicke, B.; Xuan, J. A.; Pagila, R.; Ohashi, Y.; Okada, T.; Kamata, Y.; Dinter, H. The Rho kinase inhibitor fasudil inhibits tumor progression in human and rat tumor models. *Mol. Cancer Ther.* **2006**, *5*, 2158−2164.

(7) Zhang, Z.; Schittenhelm, J.; Meyermann, R.; Schluesener, H. J. Lesional accumulation of RhoA(+) cells in brains of experimental autoimmune encephalomyelitis and multiple sclerosis. *Neuropathol. Appl. Neurobiol.* **2008**, *34*, 231−240.

(8) Oka, M.; Fagan, K. A.; Jones, P. L.; McMurtry, I. F. Therapeutic potential of RhoA/Rho kinase inhibitors in pulmonary hypertension. *Br. J. Pharmacol.* **2008**, *155*, 444−454.

(9) Hu, E.; Lee, D. Rho kinase inhibitors as potential therapeutic agents for cardiovascular diseases. *Curr. Opin. Invest. Drugs* **2003**, *4*, 1065−1075.

(10) Guagnini, F.; Ferazzini, M.; Grasso, M.; Blanco, S.; Croci, T. Erectile properties of the Rho-kinase inhibitor SAR407899 in diabetic animals and human isolated corpora cavernosa. *J. Transl. Med.* **2012**, *10*, 59−69.

(11) Liao, J. K.; Seto, M.; Noma, K. Rho kinase (ROCK) inhibitors. *J. Cardiovasc. Pharmacol.* **2007**, *50*, 17−24.

(12) Takami, A.; Iwakubo, M.; Okada, Y.; Kawata, T.; Odai, H.; Takahashi, N.; Shindo, K.; Kimura, K.; Tagami, Y.; Miyake, M.; Fukushima, K.; Inagaki, M.; Amano, M.; Kaibuchi, K.; Iijima, H. Design and synthesis of Rho kinase inhibitors (I). *Bioorg. Med. Chem.* **2004**, *12*, 2115−2137.

(13) Stavenger, R.; Cui, H.; Dowdell, S.; Franz, R.; Gaitanopoulos, D.; Goodman, K.; Hilfiker, M.; Ivy, R.; Leber, J.; Marino, J.; Oh, H.; Viet, A.; Xu, W.; Ye, G.; Zhang, D.; Zhao, Y.; Jolivette, L.; Head, M.; Semus, S.; Elkins, P.; Kirkpatrick, R.; Dul, E.; Khandekar, S.; Yi, T.; Jung, D.; Wright, L.; Smith, G.; Behm, D.; Doe, C.; Bentley, R.; Chen, Z.; Hu, E.; Lee, D. Discovery of aminofurazan-azabenzimidazoles as inhibitors of Rho-kinase with high kinase selectivity and antihypertensive activity. *J. Med. Chem.* **2007**, *50*, 2−5.

(14) Schirok, H.; Kast, R.; Figueroa-Pérez, S.; Bennabi, S.; Gnoth, M. J.; Feurer, A.; Heckroth, H.; Thutewohl, M.; Paulsen, H.; Knorr, A.; Hütter, J.; Lobell, M.; Münter, K.; Geiβ, V.; Ehmke, H.; Lang, D.; Radtke, M.; Mittendorf, J.; Stasch, J. P. Design and synthesis of potent and selective azaindole-based Rho kinase (ROCK) inhibitors. *ChemMedChem* **2008**, *3*, 1893−1904.

(15) Ho, K.; Beasley, J.; Belanger, L.; Black, D.; Chan, J. H.; Dumm, D.; Hu, B.; Klon, A.; Kultgen, S.; Ohlmeyer, M.; Parlato, S.; Ray, P.; Pharm, Q.; Rong, Y.; Roughton, A.; Walker, T.; Wright, J.; Xu, K.; Xu, Y.; Zhang, L.; Webb, M. Triazine and pyrimidine based ROCK inhibitors with efficacy in spontaneous hypertensive rat model. *Bioorg. Med. Chem. Lett.* **2009**, *19*, 6027−6031.

(16) Pireddu, R.; Forinash, K. D.; Sun, N. N.; Martin, M. P.; Sung, S. S.; Alexander, B.; Zhu, J. Y.; Guida, W. C.; Schonbrunn, E.; Sebti, S. M.; Lawrence, N. J. Pyridylthiazole-based ureas as inhibitors of Rho associated protein kinases (ROCK1 and 2). *Med. Chem. Commun.* **2012**, *3*, 699−709.

(17) LoGrasso, P.; Feng, Y. Rho kinase (ROCK) inhibitors and their application to inflammatory disorders. *Curr. Top. Med. Chem.* **2009**, *9*, 704−723.

(18) Waki, M.; Yoshida, Y.; Oka, T.; Azuma, M. Reduction of intraocular pressure by topical administration of an inhibitor of the Rho-associated protein kinase. *Curr. Eye Res.* **2001**, *22*, 470−474.

(19) Tokusbige, H.; Inatani, M.; Nemoto, S.; Sakaki, H.; Katayama, K.; Uebata, M.; Tanibara, H. Effects of topical administration of Y-39983, a selective Rho-associated protein kinase inhibitor, on ocular tissues in rabbits and monkeys. *Invest. Ophthalmol. Vis. Sci.* **2007**, *48*, 3216−3222.

(20) Nishio, M.; Fukunaga, T.; Sugimoto, M.; Ikesugi, K.; Sumi, K.; Hidaka, H.; Uji, Y. The effect of the H-1152p, a potent Rho-associated coiled coil-formed protein kinase inhibitor, in rabbit normal and ocular hypertensive eyes. *Curr. Eye Res.* **2009**, *34*, 282−286.

(21) Tanihara, H.; Inatani, M.; Honjo, M.; Tokushige, H.; Azuma, J.; Araie, M. Intraocular pressure-lowering effects and safety of topical administration of a selective ROCK inhibitor, SNJ-1656, in healthy volunteers. *Arch. Ophthalmol.* **2008**, *126*, 309−315.

(22) Yin, Y.; Cameron, M.; Lin, L.; Khan, S.; Schröter, T.; Grant, W.; Pocas, J.; Chen, Y. T.; Schürer, S.; Pachori, A.; LoGrasso, P.; Feng, Y. Discovery of potent and selective urea-based ROCK inhibitors and their effects on intraocular pressure in rats. *ACS Med. Chem. Lett.* **2010**, *1*, 175−179.

(23) Feng, Y.; Yin, Y.; Weiser, A.; Griffin, E.; Cameron, M.; Lin, L.; Ruiz, C.; Schürer, S. C.; Inoue, T.; Rao, V.; Schröter, T.; LoGrasso, P. V. Discovery of substituted 4-(pyrazol-4-yl)-phenyl-benzodioxane-2-carboxamides as potent and highly selective Rho kinase (ROCK-II) inhibitors. *J. Med. Chem.* **2008**, *51*, 6642−6645.

(24) Chen, Y. T.; Bannister, T. D.; Weiser, A.; Griffin, E.; Lin, L.; Ruiz, C.; Cameron, M.; Schürer, S.; Duckett, D.; Schröter, T.; LoGrasso, P. V.; Feng, Y. Chroman-3-amides as potent Rho kinase inhibitors. *Bioorg. Med. Chem. Lett.* **2008**, *18*, 6406−6409.

(25) Sessions, E. H.; Yin, Y.; Bannister, T. D.; Weiser, A.; Griffin, E.; Pocas, J.; Cameron, M.; Ruiz, C.; Lin, L.; Schürer, S. C.; Schröter, T.; LoGrasso, P. V.; Feng, Y. Benzimidazole-and benzoxazole-based inhibitors of Rho kinase. *Bioorg. Med. Chem. Lett.* **2008**, *18*, 6390−6393.

(26) Yin, Y.; Lin, L.; Ruiz, C.; Cameron, M.; Pocas, J.; Grant, W.; Schröter, T.; Chen, W.; Duckett, D.; Schürer, S.; LoGrasso, P. V.; Feng, Y. Benzothiazoles as Rho-associated kinase (ROCK-II) inhibitors. *Bioorg. Med. Chem. Lett.* **2009**, *19*, 6686−6690.

(27) Fang, X.; Yin, Y.; Chen, Y. T.; Yao, L.; Wang, B.; Cameron, M.; Lin, L.; Khan, S.; Ruiz, C.; Schröter, T.; Grant, W.; Weiser, A.; Pocas, J.; Pachori, A.; Schürer, S.; LoGrasso, P.; Feng, Y. Tetrahydroisoquinoline derivatives as highly selective and potent Rho kinase inhibitors. *J. Med. Chem.* **2010**, *53*, 5727−5737.

(28) Chowdhury, S.; Sessions, E. H.; Pocas, J. R.; Grant, W.; Schröter, T.; Lin, L.; Ruiz, C.; Cameron, M. D.; Schuerer, S.; LoGrasso, P. V.; Bannister, T. D.; Feng, Y. Discovery and optimization of indoles and 7-azaindoles as Rho kinase (ROCK) inhibitors (part-I). *Bioorg. Med. Chem. Lett.* **2011**, *21*, 7107−7112.

(29) Sessions, E. H.; Chowdhury, S.; Yin, Y.; Pocas, J. R.; Grant, W.; Schroeter, T.; Lin, L.; Ruiz, C.; Cameron, M. D.; LoGrasso, P. V.; Bannister, T. D.; Feng, Y. Discovery and optimization of indoles and

7-azaindoles as Rho kinase (ROCK) inhibitors (part-II). *Bioorg. Med. Chem. Lett.* **2011**, *21*, 7113−7118.
(30) Fang, X.; Chen, Y. T.; Sessions, E. H.; Chowdhury, S.; Vojkovsky, T.; Yin, Y.; Pocas, J. R.; Grant, W.; Schröter, T.; Lin, L.; Ruiz, C.; Cameron, M. D.; LoGrasso, P. V.; Bannister, T. D.; Feng, Y. Synthesis and biological evaluation of 4-quinazolinones as Rho kinase inhibitors. *Bioorg. Med. Chem. Lett.* **2011**, *21*, 1844−1848.
(31) Chowdhury, S.; Chen, Y. T.; Fang, X.; Grant, W.; Pocas, J. R.; Cameron, M. D.; Ruiz, C.; Lin, L.; Park, H.; Schröter, T.; Bannister, T. D.; LoGrasso, P. V.; Feng, Y. Rock-II Inhibitors Based on Amino Acid Derived Qinazolines. *Bioorg. Med. Chem. Lett.* **2013**, *23*, 1592−1599.
(32) Schröter, T.; Griffin, E.; Weiser, A.; Feng, Y.; LoGrasso, P. Detection of myosin light chain phosphorylation-A cell-based assay for screening Rho-kinase inhibitors. *Biochem. Biophys. Res. Commun.* **2008**, *374*, 356−360.
(33) For example, compound **1y** in ref 22 had a clearance of Cl = 61 mL/min·kg, a half-life of $t_{1/2}$ = 0.7 h, an area under curve of AUC = 0.6 μM·h, and an oral bioavailability of %F = 0.
(34) Schröter, T.; Minond, D.; Weiser, A.; Dao, C.; Habel, J.; Spicer, T.; Chase, P.; Baillargeon, P.; Scampavia, L.; Schürer, S.; Chung, C.; Mader, C.; Southern, M.; Tsinoremas, N.; LoGrasso, P.; Hodder, P. Comparison of miniaturized time-resolved fluorescence resonance energy transfer and enzyme-coupled luciferase high-throughput screening assays to discovery inhibitors of Rho-kinase II (ROCK-II). *J. Biomol. Screen.* **2008**, *13*, 17−28.
(35) Vaasa, A.; Viil, I.; Enkvist, E.; Viht, K.; Raidaru, G.; Lavogina, D.; Uri, A. High-affinity bisubstrate probe for fluorescence anisotropy binding/displacement assays with protein kinases PKA and ROCK. *Anal. Biochem.* **2009**, *385*, 85−93.